CONVOLUTION SPLINE APPROXIMATIONS FOR TIME DOMAIN BOUNDARY INTEGRAL EQUATIONS

PENNY J. DAVIES AND DUGALD B DUNCAN

ABSTRACT. We introduce a new "convolution spline" temporal approximation of time domain boundary integral equations (TDBIEs). It shares some properties of convolution quadrature (CQ) but, instead of being based on an underlying ODE solver, the approximation is explicitly constructed in terms of compactly supported basis functions. This results in sparse system matrices and makes it computationally more efficient than using the linear multistep version of CQ for TDBIE time-stepping. We use a Volterra integral equation (VIE) to illustrate the derivation of this new approach: at time step $t_n = nh$ the VIE solution is approximated in a backwards-in-time manner in terms of basis functions ϕ_j by $u(t_n - t) \approx \sum_{j=0}^{n} u_{n-j}\, \phi_j(t/h)$ for $t \in [0, t_n]$. We show that using isogeometric B-splines of degree $m \geq 1$ on $[0, \infty)$ in this framework gives a second order accurate scheme, but cubic splines with the parabolic runout conditions at $t = 0$ are fourth order accurate. We establish a methodology for the stability analysis of VIEs and demonstrate that the new methods are stable for non-smooth kernels which are related to convergence analysis for TDBIEs, including the case of a Bessel function kernel oscillating at frequency $\mathcal{O}(1/h)$. Numerical results for VIEs and for TDBIE problems on both open and closed surfaces confirm the theoretical predictions.

1. Introduction. Convolution quadrature (CQ) time-stepping for time-dependent boundary integral equations (TDBIEs) was first proposed and analyzed by Lubich in 1994 [**31**]. Since then, the inherent stability and ease of implementation of CQ (as compared to a full space-time Galerkin approximation) has made it a very popular

choice for TDBIE problems–a search on "`convolution quadrature`,"
"`boundary`" in the Thomson Reuters Web of Science database yields
nearly 200 hits. Unfortunately there is a drawback: the effective sup-
port of the time basis functions $\phi_j(t)$ which underpin CQ increases
with j, and this increases the computational complexity of the solution
algorithm. Here we describe a new "convolution spline" approxima-
tion framework which shares some properties with CQ but is explicitly
constructed in terms of compactly supported basis functions which are
(mainly) translates; this makes it easy to implement and computation-
ally efficient. We apply it to the TDBIE problem

$$(1.1) \qquad \frac{1}{4\pi} \int_\Gamma \frac{u(\vec{x}', t - |\vec{x}' - \vec{x}|)}{|\vec{x}' - \vec{x}|} \, d\vec{x}' = a(\vec{x}, t) \quad \text{for } \vec{x} \in \Gamma, \, t > 0$$

for u; this is the single layer potential equation for acoustic scattering
from the surface $\Gamma \subset \mathbb{R}^3$ with zero Dirichlet boundary conditions and
(known) incident field $-a(\vec{x}, t)$, which is equivalent to

$$\int_0^t \int_\Gamma k(\vec{x}' - \vec{x}, t - t') \, u(\vec{x}', t') \, d\vec{x}' \, dt' = a(\vec{x}, t) \quad \text{for } k(\vec{z}, t) = \frac{\delta(t - |\vec{z}|)}{4\pi |\vec{z}|}.$$

We use the convolution-kernel Volterra integral equation (VIE)

$$(1.2) \qquad \int_0^t K(t') \, u(t - t') \, dt' = a(t), \quad t \in [0, T]$$

to illustrate the derivation of the new approximation method and its
convergence and stability properties. However, the focus of the paper
is not on deriving new methods for VIEs (of which there are already
very many), but on using the insight gained from VIEs to derive new
methods which have good properties for TDBIEs.

1.1. Properties of TDBIE approximations. Designing a good
approximation scheme for the TDBIE (1.1) is nontrivial; challenges
include ensuring that it is numerically stable, it is not prohibitively hard
to implement for a given scattering surface Γ, and its computational
complexity is not infeasibly high. We begin by briefly summarizing the
pros and cons of some of the main approaches (see also [**9, 22**]).

Bamberger and Ha Duong [**1**] proved that a full Galerkin approxi-
mation of (1.1) in time and space is stable and convergent for smooth,
closed Γ (this was extended to the case of open, flat Γ in [**21**]), but the

stability of the method relies on all the integrals being evaluated very accurately (the key insight on how to do this was provided by Terrasse [**39**]). In practice this involves converting five-dimensional volume integrals over irregular (non-polygonal) sub-regions of $\Gamma \times \Gamma \times [0,T]$ to surface integrals which are then evaluated using high precision quadrature and is extremely complicated to successfully implement in practice, even for relatively simple Γ. Collocation schemes for (1.1) are far more straightforward to implement, but there is little rigorous convergence analysis for them, and numerical instability is often an issue. As noted above, methods which use a Galerkin approximation in space and CQ in time have obvious attractions: they are based on rigorous theoretical analysis [**1, 31**] (see also [**16**] for some new bounds) and are relatively straightforward to implement. They are also inherently far more stable than those which use Galerkin or collocation time approximations (Lubich showed in [**31**] that the CQ method remains stable when the inner product integrals are approximated), but unfortunately the disadvantage this time is higher computational complexity.

All three approaches approximate (1.1) as a convolution sum of the form $\sum_{j=0}^{n} \mathsf{Q}^j \, \underline{U}^{n-j} = \underline{a}^n$, which is rearranged to give the time-stepping scheme

$$(1.3) \qquad \mathsf{Q}^0 \, \underline{U}^n = \underline{a}^n - \sum_{j=1}^{n} \mathsf{Q}^j \, \underline{U}^{n-j}$$

for $\underline{U}^n \in \mathbb{R}^{N_S}$, the representation of the spatial approximation of u at or near time $t^n = n\,h$, where the right-hand side vector $\underline{a}^n$ is derived from $a(\vec{x}, t)$. In the case of both Galerkin and collocation approximations the matrices $\mathsf{Q}^j \in \mathbb{R}^{N_S \times N_S}$ are sparse–the number of nonzero elements per row of matrix Q^j is $\mathcal{O}(\min\{j, N_S^{1/2}\})$. In particular, this means that (1.3) can be solved in $\mathcal{O}(N_S^{3/2})$ operations once the right-hand side is known, and the overall computational complexity to obtain the approximate solution up to time $N_T\,h$ is $\mathcal{O}(\min\{N_T^3\,N_S, N_T^2\,N_S^{3/2}\})$ operations. For these hyperbolic problems, it is usual to use a timestep h commensurate with the side Δx of a typical space mesh element, and in this case $N_T \approx N$ and $N_S \approx N^2$ for $N = 1/\Delta x$, and the total computational complexity is $\mathcal{O}(N^5)$. Although this compares somewhat unfavourably with the $\mathcal{O}(N^4)$ computational complexity of a finite difference or finite element approximation of the PDE formulation of the acoustic wave equation in $\mathbb{R}^3$, the plane wave "fast" methods

developed by Michielssen and co-workers [**17, 18, 29**] reduces the complexity to $\mathcal{O}(N^3 \log^2 N)$.

Using CQ in time results in a solution algorithm (1.3) in which the matrices Q^j are dense, because the underlying basis functions are global (see, e.g., Section 2 below, or [**2, 23**] for more details), which increases the computational complexity to $\mathcal{O}(N_S^2 N_T^2)$. The issue is not solving (1.3) for $\underline{U}^n$ (which can typically be done efficiently by approximating Q^0 appropriately), but in performing the matrix-vector products needed to calculate the right-hand side. Lubich explains that the technique of [**24**] can be used to reduce the overall complexity to $\mathcal{O}(N_S^2 N_T \log^2 N_T)$, i.e., $\mathcal{O}(N^5 \log^2 N)$. A cut-off strategy for replacing small matrix entries by zero is described and analyzed in [**23**], and this reduces the storage costs of the method. This is combined with panel clustering in [**26**] to further reduce the storage costs. However, because the effective support of the time basis functions increases with the index (see Figure 2 or [**13**, Figure 2.2]), the computational complexity is a factor of $\sqrt{N}$ higher than that for approximations which use local basis functions.

CQ methods which are based on underlying Runge-Kutta ODE solvers have also been developed and analyzed for TDBIEs [**3, 4**]. There are several advantages of these methods over linear multistep CQ methods: the basis functions are more highly concentrated [**2**, Figures 1, 2], which makes sparsifying the Q^j matrices more straightforward; and higher order accurate methods in time are possible. Banjai [**2**] uses this approach to develop a practical, parallelizable solution algorithm for (1.1) which he illustrates with a number of realistic large-scale numerical examples.

1.2. New convolution spline methods. The Q^j system matrices in (1.3) for our new method have the same sparsity pattern as for the Galerkin or collocation approximations described above, and so it is considerably more efficient (both to set up by calculating the system matrices, and to run) than using the linear multistep version of CQ. Our method gives a TDBIE solution scheme whose overall complexity is $\mathcal{O}(\min\{N_T^3 N_S, N_T^2 N_S^{3/2}\}) = \mathcal{O}(N^5)$ operations (and which could also be potentially speeded up using fast methods). It is also far easier to implement than the full space-time Galerkin approach.

We derive the new approximation as a solution method for the VIE (1.2), with u approximated in terms of B-spline basis functions in a backwards-in-time framework. Our initial approach is to use isogeometric B-splines of degree m on $[0, \infty)$. There can be advantages in using higher order values of m even though the formal convergence rate of this scheme for a smooth VIE problem is limited to second order (because it is based on quasi-interpolation by the Schoenberg B-spline operator). For example, as noted in [**36**], using smooth temporal basis functions greatly simplifies approximating the integrals in (1.1). We also consider cubic B-splines with the parabolic runout condition at $t = 0$ and show that these are fourth order accurate. We carefully test out the new methods on (1.2), establishing formal convergence, and examining the behavior for kernels which mimic some of the important properties of TDBIE problems, such as discontinuous step-function kernels (see, e.g., [**37**]). Another important test problem is obtained from taking the spatial Fourier transform of (1.1) at frequency $\vec{\omega} \in \mathbb{R}^2$ when $\Gamma = \mathbb{R}^2$. This is

$$(1.4) \qquad \int_0^t J_0(\omega t')\, \widehat{u}(\vec{\omega}, t - t')\, dt' = 2\widehat{a}(\vec{\omega}, t),$$

where $\omega = |\vec{\omega}|$ and J_0 is the first kind Bessel function of order zero. As noted in [**10**], instabilities of approximation schemes for (1.1) are typically exhibited at the highest spatial frequency which can be represented on the mesh. Hence, it is important to ensure that any prototype numerical scheme for time-stepping (1.1) is stable for (1.4) at values of $\omega = \mathcal{O}(1/h)$ (assuming $h \approx \Delta x$).

1.3. Outline. Section 2 contains an alternative derivation of Lubich's [**30**] CQ method for (1.2) in terms of basis functions which have the sum to unity property (2.12). The new convolution spline approximation of (1.2) is described in Section 3 in terms of basis functions which have compact support and are (essentially) all translates, and we give sufficient conditions for this approximation to be stable. We consider the case in which the basis functions are mth degree isogeometric B-splines on $[0, \infty)$ in Section 4, showing how Laplace transform techniques can be used to prove the stability of this approximation of (1.2) for several different test kernels, and demonstrating second order convergence for (1.2) when K and a satisfy

$$(1.5) \quad a \in C^{d+1}[0, T], \quad K \in C^{d+1}[0, T], \quad a(0) = 0 \text{ and } K(0) = 1$$

for suitable $d \geq 0$. Under these assumptions, equation (1.2) possesses a unique solution $u \in C^d[0, T]$, e.g., see [**6**, Theorem 2.1.9].

In Section 5, we consider a cubic convolution spline basis which is modified near $t = 0$ to satisfy the parabolic runout conditions and show that this gives a far more stable approximation of (1.2) which is fourth order convergent. Numerical tests show that it achieves fourth order accuracy even for a discontinuous kernel. We present numerical test results for TDBIEs in Section 6 which use a Galerkin approximation in space (based on triangular piecewise constant elements), and the new cubic convolution spline basis in time, for both open and closed surfaces Γ. These show that the new scheme performs far better than CQ based on BDF2–it is both more accurate and more efficient.

The TDBIE test problems are similar to those considered in [**13**] which use the convolution-in-time framework with non-polynomial (global) basis functions, but the modified B-spline basis functions give a more accurate temporal approximation. We note that the time-stepping schemes of [**13**] rely on the theoretical framework developed in Sections 2–3 of the present work.

2. CQ based on linear multistep methods for (1.2). We begin by outlining Lubich's derivation [**30**] of the CQ method for (1.2) in order to show how it can be reinterpreted in terms of CQ basis functions. For simplicity we restrict attention to the case for which the extension of the solution u by zero to the negative real axis is in $C^d(-\infty, T]$ (otherwise the CQ method needs to be 'corrected' as described in [**30**, Section 3] in order to attain optimal convergence). This is guaranteed by requiring

$$(2.1) \qquad\qquad a^{(p)}(0) = 0 \quad \text{for } p = 0 : d + 1$$

because $u^{(p)}(0) = a^{(p+1)}(0) - \sum_{\ell=0}^{p-1} K^{(p-\ell)}(0)\, u^{(\ell)}(0)$. We also assume that the Laplace transform $\overline{K}(s)$ of the kernel K is sufficiently well-behaved for all the formal manipulations in the next subsection to be rigorous. For details, see for example, [**2**, App] or [**31**, Section 1].

2.1. Lubich's CQ method. We follow Lubich [30] and substitute the Laplace inversion formula for $\overline{K}(s)$ into (1.2) to obtain

$$(2.2) \qquad a(t) = \frac{1}{2\pi i} \int_\gamma \overline{K}(s)\, y(t,s)\, ds,$$

where γ is an infinite contour within the region of analyticity of $\overline{K}(s)$ and

$$y(t,s) = \int_0^t e^{st'}\, u(t - t')\, dt'.$$

Treating the Laplace variable s as a parameter, $y(t)$ solves the ODE:

$$(2.3) \qquad \dot{y}(t) = s\, y(t) + u(t), \quad y(0) = 0,$$

and this is approximated by the k-step ($k \leq d$) linear multistep method with timestep h

$$(2.4) \qquad \sum_{j=0}^k \alpha_j\, y_{n+j-k} = h \sum_{j=0}^k \beta_j\, f_{n+j-k},$$

where $t_n = nh$, $y_n \approx y(t_n)$ and $f_n = s\, y_n + u(t_n)$. The starting values are $y_{-k} = \cdots y_{-1} = 0$ because of the assumption (2.1). Multiplying (2.4) by ξ^n and summing over n (for $\xi \in \mathbb{C}$ for which the sum converges) gives

$$\left(\frac{\delta(\xi)}{h} - s \right) \sum_{n=0}^\infty y_n\, \xi^n = \sum_{n=0}^\infty u(t_n)\, \xi^n,$$

where

$$\delta(\xi) = \sum_{j=0}^k \alpha_j\, \xi^{k-j} \Big/ \sum_{j=0}^k \beta_j\, \xi^{k-j}$$

is the symbol of (2.4). Hence, y_n is the coefficient of ξ^n in the expansion of $(\delta(\xi)/h - s)^{-1} \sum_{k=0}^\infty u(t_k)\, \xi^k$. Substituting y_n for $y(t_n)$ in (2.2) shows that $a(t_n)$ is approximated by the coefficient of ξ^n in

$$\frac{1}{2\pi i} \int_\gamma \left(\frac{\delta(\xi)}{h} - s \right)^{-1} \overline{K}(s)\, ds \sum_{k=0}^\infty u(t_k)\, \xi^k = \overline{K}(\delta(\xi)/h) \sum_{k=0}^\infty u(t_k)\, \xi^k$$

using Cauchy's integral formula. Hence, defining the CQ weights $q_k = q_k(h)$ to be the coefficients in the expansion

$$(2.5) \qquad \overline{K}(\delta\,(\xi)/h) = \sum_{k=0}^{\infty} q_k\,\xi^k$$

gives the CQ approximation of (1.2)

$$(2.6) \qquad a(t_n) = \sum_{j=0}^{n} q_j\,u_{n-j}.$$

This can be rearranged to give the time-stepping approximate solution $u_n \approx u(t_n)$

$$(2.7) \qquad u_n = \frac{1}{q_0}\left(a(t_n) - \sum_{j=1}^{n-1} q_j\,u_{n-j}\right) \quad \text{for } n \geq 1,$$

since, by assumption, $u_0 = u(0) = 0$.

2.2. Derivation of CQ in terms of basis functions. The CQ approximation scheme (2.6) for the VIE (1.2) is defined solely in terms of the weights q_k. But, if CQ is used to time-step a TDBIE, then the approximation involves CQ basis functions, see e.g., **[2, 23, 32]**. However, we are not aware of a general interpretation of CQ approximation schemes for (1.2) in terms of basis functions. As well as yielding some interesting observations, this also gives the framework which we use for the derivation of our convolution spline methods in Sections 4–5.

At $t = t_n := nh$, (1.2) can be written as

$$(2.8) \qquad a(t_n) = \int_0^{\infty} K(t')\,u(t_n - t')\,dt',$$

because $u(t) = 0$ for $t \leq 0$. We show below that the standard CQ method is equivalent to approximating u in (2.8) by

$$(2.9) \qquad u(t_n - t') \approx \sum_{j=0}^{n} u_{n-j}\phi_j(t'/h) \quad \text{for } t' \geq 0,$$

where ϕ_j are basis functions, i.e., the approximation at t_n is $U_n(t) = \sum_{k=0}^{n} u_k\,\phi_{n-k}(n - t/h)$ for $t \leq t_n$. Note that $\phi_{n-k}(n - t/h)$ depends

on n, i.e., CQ is *fundamentally different* from a standard finite-element type approximation in which an unknown coefficient is always associated with the same basis function.

Substituting (2.9) into (2.8) and comparing the resulting expression with (2.6) gives the relationship between the standard CQ weights and basis functions:

$$(2.10) \qquad q_j = \int_0^\infty K(t)\, \phi_j(t/h)\, dt\,.$$

Comparing this with the standard CQ definition of q_j in (2.5) gives (see [2, Equation (3.1)])

$$(2.11) \qquad e^{-\delta(\xi)t} = \sum_{j=0}^\infty \phi_j(t)\, \xi^j\,.$$

An immediate consequence is that the basis functions satisfy the sum to unity property

$$(2.12) \qquad \sum_{j=0}^\infty \phi_j(t) = 1,$$

provided the underlying multistep ODE solver is consistent, because in this case $\delta(1) = 0$. This new observation is a crucial property which we use in Section 3.

2.3. CQ basis functions for LMMs. Explicit formulae for the $\phi_j(t)$ based on BDF1-2 have been used for TDBIE approximations [23, 32]. The formula for BDF1 is given in [32], and in this case, $\phi_j(t) = e^{-t}\, t^j/j!$, i.e., they are Erlang functions, used in statistics as probability density functions and satisfy $\phi_j(t) \geq 0$ and $\int_0^\infty \phi_j(t)\, dt = 1$. The derivation for BDF2 is more complicated, and the explicit formula

$$\phi_j(t) = \frac{1}{j!}\, H_j(\sqrt{2t}) \left(\frac{t}{2} \right)^{j/2} e^{-3t/2}$$

is given in [23], where H_j is the jth Hermite polynomial. Note that the properties of H_j imply that $\phi_j(t)$ involves a jth degree polynomial and an exponential in t with no fractional powers of t.

In principle, (2.11) can be used directly to find the basis functions $\phi_j(t)$ corresponding to any underlying linear multistep ODE method

for (2.3), although this may not be easy in practice. For the trapezoidal rule $\delta(\xi) = 2\,(1-\xi)/(1+\xi)$ [2] ,and (2.11) is $\sum_{j=0}^{\infty} \phi_j(t)\,\xi^j = e^{-2t}\,f(\xi)$, where $f(\xi) = \exp(4\,t/(1+\xi))$. This gives $f(\xi) = \sum_{j=0}^{\infty} f_j\,\xi^j$ where

$$f_j = \frac{1}{j!}\frac{d^j}{d\xi^j}\,f(\xi)\bigg|_{\xi=0} = \frac{1}{j!(4t)^j}\frac{d^j}{dz^j}\,e^{-1/z}\bigg|_{z=1/(4t)}$$

using the change of variables $z = (1 + \xi)/(4t)$. It follows from [33, equation 18.5.6] that $f_j = (-1)^j e^{-4t}\,L_j^{-1}(4t)$, where $L_j^{\alpha}(x)$ is a Laguerre polynomial. The identity $L_j^{-1}(x) = L_j(x) - L_{j-1}(x)$ [20, equations 8.971–5] gives the trapezoidal rule basis functions $\phi_j(t) = (-1)^j\{\ell_j(4\,t) - \ell_{j-1}(4t)\}$, where $\ell_j(x) = e^{-x/2}\,L_j(x)$ is the jth Laguerre function. They are oscillatory but do satisfy $\int_0^{\infty} \phi_j(t)\,dt = 1$. The low order basis functions are shown in Figure 1 (see also [2, Figure 1] and [32, Figure 4]). Figure 2 shows how the CQ basis functions spread out as j increases; this increases the number of non-zero entries in the $\mathbf{Q}^j$ matrices of (1.3) and makes CQ time-stepping less efficient.
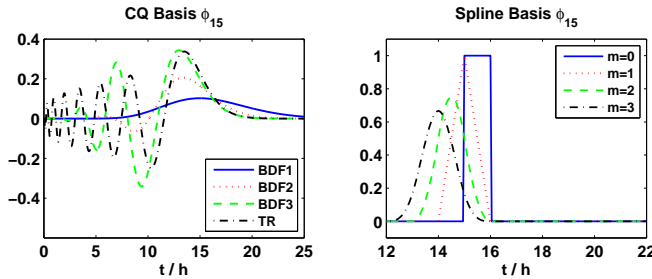

FIGURE 1. Typical CQ and spline basis functions. See subsections 2.3 and 4.1 for details.

The direct approach appears intractible for more complicated schemes (even for BDF3), and recurrence relations for the basis functions are given in [32, subsection 3.2]. They can be compactly derived by formally differentiating the generating function (2.11) with respect to ξ to get

$$\sum_{j=1}^{\infty} j\phi_j(t)\,\xi^{j-1} + t\delta'(\xi)\sum_{j=0}^{\infty} \phi_j(t)\,\xi^j = 0,$$
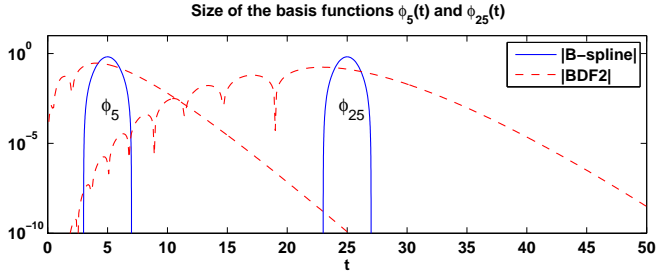
FIGURE 2. Basis functions $\phi_5(t)$ and $\phi_{25}(t)$ for CQ (BDF2) compared with cubic splines (from Sec. 5). The effective support of the CQ basis functions $\phi_j(t)$ increases with j.

Scheme	Initial $\phi_{-n} \equiv 0, n \geq 1$	Recurrence for basis functions $j \geq 1$
BDF1	$\phi_0(t) = e^{-t}$	$j\phi_j(t) - t\phi_{j-1}(t) = 0$
BDF2	$\phi_0(t) = e^{-3t/2}$	$j\phi_j(t) - 2t\phi_{j-1}(t) + t\phi_{j-2}(t) = 0$
BDF3	$\phi_0(t) = e^{-11t/6}$	$j\phi_j(t) - 3t\phi_{j-1}(t) + 3t\phi_{j-2}(t) - t\phi_{j-3}(t) = 0$
BDF4	$\phi_0(t) = e^{-25t/12}$	$j\phi_j(t) - 4t\phi_{j-1}(t) + 6t\phi_{j-2}(t) - 4t\phi_{j-3}(t)$ $+t\phi_{j-4}(t) = 0$
Trap. rule	$\phi_0(t) = e^{-2t}$	$j\phi_j(t) - 4t\phi_{j-1}(t) + 2(j-1)\phi_{j-1}(t)$ $+(j-2)\phi_{j-2}(t) = 0$

TABLE 1. Recurrence relations for the CQ basis functions.

and then collecting terms in ξ. The initial conditions are $\phi_n(t) \equiv 0$ for $n < 0$, and the first term of the Taylor expansion of (2.11) gives $\phi_0(t) = e^{-\delta(0)t} = e^{-\delta_0 t}$. Recurrence relations for BDF1–4 and the trapezoidal rule are given in Table 1.

3. Convolution spline approach. As discussed in Section 1, basis functions with global support (such as those described above) give rise to dense matrices $\mathbf{Q}^j$ in the TDBIE scheme (1.3), and this has storage and computational cost implications. Here we explore the use of compactly supported basis functions, which although not derived via standard CQ, nevertheless do fit into the CQ form (2.9). We set up a general framework for basis functions for the VIE (1.2) which are (mainly) translates, and consider specific examples based on B-splines

in Sections 4–5. This new approach gives sparse system matrices when used to time-step TDBIEs, and results are presented in Section 6. It also provides the underpinning theoretical framework for the TDBIE time-stepping approximations of [**13**].

3.1. Construction of a convolution spline scheme for (1.2). We consider approximations of the form (2.9), but where all the basis functions ϕ_j have compact support of width $\mathcal{O}(h)$ and almost all are translates of a standard, compactly supported basis function ϕ_m, i.e.,

$$(3.1) \qquad \phi_j(t/h) = \phi_m(t/h + m - j) \quad \text{for } j \geq m.$$

When the basis functions are splines, then m is also equal to the polynomial degree.

Property (3.1) means that the approximation $U(t_n - t) \approx u(t_n - t)$ has the form

$$(3.2) \qquad U(t_n - t) = \sum_{j=0}^{m-1} v_{n-j}\phi_j\left(\frac{t}{h}\right) + \sum_{j=m}^{n} v_{n-j}\,\phi_m\left(\frac{t}{h} + m - j\right)$$

for $t \geq 0$, where v_j approximates $u(t)$ for t near (but not necessarily at) t_j, and a sum is defined to be zero if its upper index is less than its lower index. Note that when *all* the ϕ_j are translates (as happens for piecewise constant or linear approximations), then $\phi_{n-k}(n-s) \equiv \phi_k(s)$ and the convolution-in-time representation (2.9) fits into a standard finite element framework.

Substituting the approximation (3.2) into the integral equation (1.2) and collocating at each time level as described in subsection 2.2 gives

$$(3.3) \qquad \sum_{j=0}^{n} q_j v_{n-j} = a(t_n)$$

for $n = 0 : N$ where the weights q_j are defined by (2.10). The unknown coefficients $\{v_j\}_{j=0}^{N}$ are then found by time marching as in (2.7). An alternative expression which is useful for analysis is $q_0 v_n = \sum_{j=0}^{n} p_j a(t_{n-j})$ for $n \geq 1$, where the stability coefficients p_n are defined recursively by

$$(3.4) \qquad p_0 = 1, \qquad p_n = \frac{-1}{q_0}\sum_{j=1}^{n} q_j p_{n-j} \quad \text{for } n \geq 1.$$

3.2. Stability of (3.3). For TDBIE applications and analysis (see, e.g., [**12**]), we require the scheme (3.3) to be stable in the following sense, independent of the input function $a(t)$.

Definition 3.1 (Stability). The scheme (3.3) is said to be stable when the impulse response sequence $\{p_n\}$ defined by (3.4) satisfies $|p_n| \le C$ for all n such that $nh \le T$, where the constant C is independent of h.

This is weaker than BIBO (bounded input bounded output) stability in the signal processing literature (see, e.g., [**35**]), which requires boundedness of the absolute sum $\sum_{n=0}^{\infty} |p_n| < \infty$.

Stability properties of the scheme (3.3) can be established by using the Z-transform, defined as follows.

Definition 3.2. The Z-transform of a sequence $\{f_n\}_{n=0}^{\infty}$ is the function F given by

$$(3.5) \qquad F(\xi) = \mathcal{Z}\{f_n\}(\xi) = \sum_{n=0}^{\infty} f_n \, \xi^n$$

where $\xi \in \mathbb{C}$ with $|\xi| \le 1$ is such that the sum converges.

The scheme (3.3) is a convolution sum, and its Z-transform is

$$(3.6) \qquad Q(\xi) \, V(\xi) = A(\xi),$$

where

$$(3.7) \qquad Q(\xi) = \sum_{j=0}^{\infty} \xi^j \int_0^{\infty} K(t) \, \phi_j(t/h) \, dt$$

and we take $a_n = a(t_n)$. The p_n coefficients satisfy $\sum_{j=0}^{n} q_j p_{n-j} = 0$ for $n \ge 1$, and when $n = 0$ this "sum" is equal to q_0 (because $p_0 = 1$), and so the Z-transform of (3.4) is $Q(\xi) \, P(\xi) = q_0$, giving $P(\xi) = q_0/Q(\xi)$. We now state a sufficient condition for stability when $Q(\xi)$ is a rational function.

Theorem 3.1 (Root condition for stability). *If the Z-transform $Q(\xi)$ of $\{q_n\}$ is a rational function in ξ, then the approximation (3.3) is stable in the sense of Definition 3.1 if the roots ξ_k of $Q(\xi)$ satisfy the*

following for any constant $c \geq 0$ (independent of h): $|\xi_k| \geq 1/(1+ch)$ and any with $1/(1+ch) \leq |\xi_k| \leq 1$ are simple.

Simple roots with $|\xi_k| = 1/(1+ch)$ make a bounded contribution to p_n as n increases by the standard result

$$|\xi_k|^{-n} = (1+ch)^n \leq e^{cT}$$

for $t_n \leq T$, but roots of this size with multiplicity $\mu \geq 2$ contribute terms which grow like $n^{\mu-1}$ and hence violate the stability definition.

Remark. Although this result is a variant of the *root condition* familiar (after the change of variable $z = 1/\xi$) from zero stability analysis of numerical methods for ODEs, we note that it does not appear to have previously been derived or used to determine the stability of VIE schemes.

Verifying the stability condition directly or via the root condition above for a general approximation scheme for (1.2) may be very complicated. But, as we show below, schemes with the translate property (3.1) can be tackled within the framework of Laplace transforms originally introduced for CQ, and this approach gives a way to extend the scope of stability analysis to a far broader range of kernel functions.

Substituting the Laplace inversion formula for K into (2.1) gives

$$q_j = \frac{h}{2\pi i} \int_\gamma \overline{K}(s)\, \Phi_j(-sh)\, ds,$$

where $\Phi_j(s)$ is the Laplace transform of ϕ_j. Hence, the approximation scheme (3.3) can be written as

$$(3.8) \qquad\qquad a(t_n) = \frac{1}{2\pi i} \int_\gamma \overline{K}(s)\, y_n(sh)\, ds$$

where

$$y_n(sh) = h \sum_{j=0}^{n} v_{n-j} \Phi_j(-sh).$$

We note that y_n plays the same role here that the approximate solution of the ODE (2.3) does in standard CQ.

The translate property (3.1) and the compact support of ϕ_m imply

$$\Phi_j(-sh) = e^{sh(j-m)}\,\Phi_m(-sh) \quad \text{for } j \geq m,$$

and so

$$y_n(sh) - e^{sh}y_{n-1}(sh) = hv_n\Phi_0(-sh)$$
$$+ h\sum_{j=1}^{m} v_{n-j}\left(\Phi_j(-sh) - e^{sh}\Phi_{j-1}(-sh)\right),$$

(using $v_j \equiv 0$, $j \leq 0$). Taking the Z-transform of this expression gives

$$Y(\xi, sh) = hB(\xi, sh)\,V(\xi)/(1 - e^{sh}\xi)$$

when $\xi \neq e^{-sh}$, where

$$(3.9) \qquad B(\xi, sh) = \Phi_0(-sh) + \sum_{j=1}^{m}\left[\Phi_j(-sh) - e^{sh}\Phi_{j-1}(-sh)\right]\xi^j.$$

It hence follows from (3.8) that

$$A(\xi) = V(\xi)\frac{h}{2\pi i}\int_{\gamma} \overline{K}(s)\left(\frac{B(\xi, sh)}{1 - e^{sh}\xi}\right) ds$$

and comparison with (3.6) yields the alternative representation for the Z-transform of the weights q_j:

$$(3.10) \qquad Q(\xi) = \frac{h}{2\pi i}\int_{\gamma} \overline{K}(s)\left(\frac{B(\xi, sh)}{1 - e^{sh}\xi}\right) ds.$$

The expression $B(\xi, sh)/(1 - e^{sh}\xi)$ plays a role similar to that of $(\delta(\xi)/h - s)^{-1}$ in standard CQ analysis, and it is the key quantity in determining whether the scheme is stable or not. Unfortunately, it has a more complicated structure: it has an infinite vertical line of simple poles at $s = s_k$ for $k \in \mathbb{Z}$, where

$$(3.11) \qquad s_k := \frac{1}{h}\left(-\ln|\xi| - i\,\mathrm{Arg}\,(\xi) + i\,2\pi k\right)$$

and the principal argument $\mathrm{Arg}\,(\xi) \in (-\pi, \pi]$. Note that, if $|\xi| < 1$, then $\mathrm{Re}\,(s_k) > 0$.

To evaluate $Q(\xi)$ defined by (3.10) for a given kernel function $K(t)$, we can use either the left or right D-contours illustrated in Figure 3,
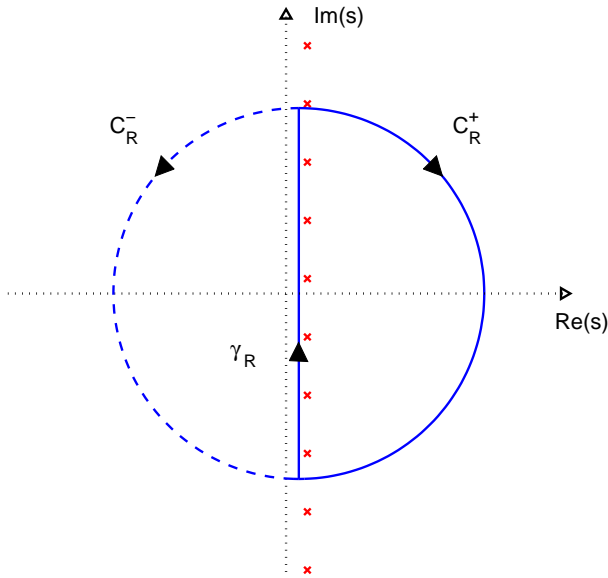
FIGURE 3. The left and right D-contours of radius R used for the stability and Z-transform calculations. The crosses are the poles (3.11) and the vertical line of length (approximately) $2R$ is γ_R.

taking the limit $R \to \infty$ and setting $\gamma = \lim_{R \to \infty} \gamma_R$. Using the right contour gives

$$Q(\xi) = \sum_{k=-\infty}^{\infty} \overline{K}(s_k)B(\xi, s_k h) - \lim_{R \to \infty} \frac{h}{2\pi i} \int_{C_R^+} \overline{K}(s) \left(\frac{B(\xi, sh)}{1 - e^{sh}\, \xi} \right) ds.$$

The integral round C_R^+ does not necessarily vanish as $R \to \infty$ since, for some basis functions (including higher order B-splines), the quantity

$$\frac{B(\xi, sh)}{1 - e^{sh}\, \xi} = \mathcal{O}(e^{csh})$$

as $\mathrm{Re}\,(s) \to \infty$ for $c \geq 1$. We may also use the left contour when $\overline{K}(s)$ has simple poles at $s = \kappa_j$ with $\mathrm{Re}\,(\kappa_j) \leq 0$ and obtain the analogous

result

$$Q(\xi) = h \sum_j \lim_{s \to \kappa_j} \left(\frac{(s - \kappa_j)B(\xi, sh)}{1 - e^{sh}\xi} \, \overline{K}(s) \right)$$

$$- \lim_{R \to \infty} \frac{h}{2\pi i} \int_{C_R^-} \overline{K}(s) \left(\frac{B(\xi, sh)}{1 - e^{sh}\,\xi} \right) ds\,.$$

The asymptotic behavior of the integral C_R^- as $R \to \infty$ is determined primarily by $\overline{K}(s)$. The extension of this left contour approach to poles with higher multiplicity is straightforward. We illustrate the use of these formulae in subsection 4.2 for various kernels K when the basis functions are B-splines.

4. B-spline basis functions for (1.2). We now illustrate the theoretical framework introduced in Section 3 for basis functions ϕ_j which are B-splines on $[0, \infty)$. We begin by listing some general properties of B-splines which are needed in the subsequent analysis and then examining the stability of the convolution spline approximation of (1.2) for different example kernels. We also prove that the approximation given by (3.3) converges to the solution u of (1.2) for general smooth a and K. The convergence rate is at most second order, no matter how high the polynomial degree, because quasi-interpolation by the Schoenberg B-spline operator is at most $\mathcal{O}(h^2)$ [14]. However, a simple modification of the B-spline basis near $t = 0$ can give higher order stable approximations of (1.2), and this is analyzed for the cubic case in Section 5.

4.1. Notation and properties. We now look in detail at the approximation (3.2) when the basis functions are (iso-geometric) B-splines of polynomial degree m based on the uniformly spaced nodes (or knots) $t_j = j\,h$ for $j \geq 0$. It is necessary for the B-spline basis functions to have the sum to unity property (2.12) in the whole interval $[0, \infty)$, and we introduce m new knots $t_j = 0$ for $j = -m : -1$. The mth degree B-splines are $b_j^m(t)$ for $j \geq -m$, and B-splines of degree $m > 0$ are recursively defined in terms of those of lower degree as follows, using the convention that $b_j^m(t) \equiv 0$ for $j < -m$.

Definition 4.1. [14] When $m = 0$,

$$b_j^0(t) = \begin{cases} 1 & \text{if } t \in [t_j, t_{j+1}) \text{ for } j \geq 0 \text{ and} \\ 0 & \text{otherwise.} \end{cases}$$

If $m > 0$, then

$$b_j^m(t) = \left(\frac{t - t_j}{t_{j+m} - t_j}\right) b_j^{m-1}(t) + \left(\frac{t_{j+m+1} - t}{t_{j+m+1} - t_{j+1}}\right) b_{j+1}^{m-1}(t)$$

where the convention is that $0/0$ is interpreted as 0.

Throughout this section, we shall use basis functions

(4.1) $$\phi_j(t/h) = b_{j-m}^m(t) \quad \text{for } j \geq 0.$$

Note that the spline degree m is also the translate parameter from (3.1).

We make use of several B-spline properties in Section 4 (see, for example, standard references such as [14, 38]), which we list here for convenience.

B-spline properties.

P1 **Compact support.** $b_j^m(t) = 0$ outwith $[t_j, t_{j+m+1})$, and $b_j^m(t_j) = 0$ unless $j = -m$.

P2 **Translate property.** If $j \geq 0$, then $b_j^m(t) = b^m(t/h - j)$, where the functions b^m are defined recursively:

$$b^0(\tau) = \begin{cases} 1 & \text{if } \tau \in [0, 1), \\ 0 & \text{otherwise,} \end{cases}$$

and if $m \geq 1$:

$$b^m(\tau) = \frac{\tau}{m} b^{m-1}(\tau) + \frac{m + 1 - \tau}{m} b^{m-1}(\tau - 1).$$

It follows that $\phi_j(\tau) = b^m(\tau + m - j)$ for $j \geq m$.

P3 **Sum to unity.** $\sum_{j=-m}^{\infty} b_j^m(t) = 1$ for all $t \geq 0$.

P4 **Moments.**

$$\int_{t_{j-m}}^{t_{j+1}} b_{j-m}^m(t)\, dt = \frac{t_{j+1} - t_{j-m}}{m + 1}$$

and

$$\int_{t_{j-m}}^{t_{j+1}} t\, b_{j-m}^m(t)\, dt = \frac{t_{j+1} - t_{j-m}}{(m+1)(m+2)} \sum_{k=0}^{m+1} t_{j-m+k}.$$

P5 **Shoenberg quasi-interpolation.** Suppose that $m \geq 1$, and set $t_j^m = [h\,(m + j)\,(m + j + 1)]/2m$ for $j = -m : -1$ and $t_j^m = t_{j+(m+1)/2}$ for $j \geq 0$. Then $\sum_{j=-m}^{\infty} t_j^m\, b_j^m(t) = t$ when $t \geq 0$.

It follows from properties P1, P3 and P5 above that

$$(4.2) \qquad f(t) = \sum_{j=-m}^{\infty} f(t_j^m)\, b_j^m(t) + \mathcal{O}(h^2)$$

for any $f \in C^2[0, \infty)$, and if $f \in C^{p+1}[0, \infty)$ for $p \geq 2$ and $t \in [t_\ell, t_{\ell+1})$ for some $\ell \geq 0$, then

$$(4.3) \quad f(t) - \sum_{j=\ell-m}^{\ell} f(t_j^m)\, b_j^m(t) = \sum_{k=2}^{p} \frac{f^{(k)}(t_\ell)}{k!}$$

$$\times \left[(t - t_\ell)^k - \sum_{j=\ell-m}^{\ell} (t_j^m - t_\ell)^k\, b_j^m(t) \right] + \mathcal{O}(h^{p+1}).$$

It follows from P1 that the CQ weights are

$$(4.4) \qquad q_j = \int_{t_{j-m}}^{t_{j+1}} K(t)\, b_{j-m}^m(t)\, dt.$$

The convergence analysis relies crucially on knowing the values of the weights when K is a constant, and this follows immediately from P4: when $K \equiv 1$, the weights q_j of (4.4) are given by

$$\frac{q_j}{h} = \begin{cases} (j+1)/(m+1) & \text{for } j = 0 : m - 1 \\ 1 & \text{if } j \geq m. \end{cases}$$

4.2. Stability results for convolution B-splines. We now use the theoretical framework introduced in Section 3 to examine the stability of the convolution B-spline approximation of (1.2) for different example kernels which capture some of the important properties of TDBIE problems. These are: $K(t)$ equal to a constant, a step function and the highly oscillatory kernels $K(t) = J_0(\omega t)$ or $\cos(\omega t)$, where ω can be of the order of $1/h$. We use $B_m(\xi, sh)$ to denote the function defined by (3.9) for the degree m basis functions, and $Q_m(\xi)$ to denote the coefficient Z-transform given by (3.10). The first few values of $B_m(\xi, sh)$ are listed in Table 2; those for higher values of m are

more complicated but are easily computed in a standard algebraic manipulation package.

In three of the cases $Q_m(\xi)$ is a rational function in ξ and Theorem 3.1 can be used to determine stability. The Bessel function case is more complicated, and stability is determined from the Z-transform inversion formula by bounding the coefficients p_n of (3.4) directly. Note that this bound is independent of n and so is a practically useful stability result, in contrast with the (essentially) uncheckable hypotheses needed in [**11**].

B-spline degree	$B_m(\xi, s)$	$\lim_{s\to 0} B_m(\xi, s)$	$B_m(e^{-s}, s)$
$m = 0$	$s^{-1}(e^s - 1)$	1	$s^{-1}(e^s - 1)$
$m = 1$	$s^{-2}\left[e^s(\xi s - \xi + 1) + (\xi - s - 1)\right]$	$(1+\xi)/2$	$s^{-2}(e^s - 1)^2 e^{-s}$
$m = 2$	$s^{-3}\left[e^{2s}(\xi^2 - \xi) + e^s(2 - 2\xi^2 s \right.$ $+\xi(s^2 + 2s - 2)) +$ $\left. ((2s+3)\xi - s^2 - 2s - 2 - \xi^2)\right]$	$(1+\xi+\xi^2)/3$	$s^{-3}(e^s - 1)^3 e^{-2s}$
$m = 3$	$s^{-4}(e^s\xi - 1)\left[s^3 - 3s^2(\xi - 1)\right.$ $+3s(\xi - 1)(\xi - 2)$ $-\frac{1}{2}(\xi - 1)(2\xi^2 - 9\xi + 12)$ $\left. +\frac{1}{2}e^s(\xi - 1)(e^s\xi - 6\xi + 10)\right]$ $+s^{-4}e^s(\xi - 1)^4$	$(1+\xi+\xi^2+\xi^4)/4$	$s^{-4}(e^s - 1)^4 e^{-3s}$

TABLE 2. The function $B_m(\xi, s)$ for $m = 0 : 3$. (See text for details.)

4.2.1. Constant kernel: $K(t) = 1$, transform $\overline{K}(s) = 1/s$. Integrating (3.10) round the left contour in Figure 3 gives

$$(4.5) \qquad Q_m(\xi) = h \lim_{s\to 0} \frac{B_m(\xi, sh)}{1 - e^{sh}\xi} = \frac{h(1 - \xi^{m+1})}{(m + 1)(1 - \xi)^2}.$$

The function Q_m has m simple roots on the unit circle, and stability of the approximation then follows from Theorem 3.1. (Note that stability also follows from the convergence result of subsection 4.3.)

4.2.2. Discontinuous step-function kernel: $K(t) = 1$ for $t \in [0, L]$, otherwise 0. Discontinuous kernels can arise in TDBIE problems, even when the scattering surface Γ is smooth and closed. Examples (in Laplace transformed representation) are given in [**3,** subsection 6.1] and [**37,** subsection 4.1] describing time domain scattering where only the zeroth order harmonic in space is excited on the surface of a sphere. Similar, but more complicated discontinuous kernels are

described in [**37**] for more general scattering from spheres involving higher spatial harmonics.

We assume that the duration L is independent of h and denote the integer part of L/h by M, i.e., when h is sufficiently small, $L = (M+r)\,h$ for integer $M > m$ and $r \in [0,1)$. It is simplest to work with the explicit Z-transform formula (3.5) using the weights given in (4.4). Results for $m = 0 : 3$ are summarized below.

Case m = 0.

$$\frac{Q_0(\xi)}{h} = r\,\xi^M + \sum_{n=0}^{M-1} \xi^n = \frac{1}{\xi - 1}\left(r\,\xi^{M+1} + (1-r)\,\xi^M - 1\right).$$

When $r \in (0,1)$, it can be shown that the M roots ξ_j of Q_0 satisfy $|\xi_j| > 1$ for $j = 1 : M$, and when $r = 0$ there are $M - 1$ simple roots $\xi_j = \exp(i2\pi j/M)$ for $j = 1 : M - 1$. Hence, Theorem 3.1 implies that the $m = 0$ scheme is stable for all L.

Case m = 1. We have

$$Q_1(\xi) = \frac{h}{2}\frac{1}{1-\xi}\left(1 + \xi - \xi^M g\right),$$

with $g(r,\xi) = \xi + (1 - r + r\xi)^2$ and $r \in [0,1)$. Using the definition (3.4) and formal power series expansion for small ξ gives

$$P_1(\xi) = \frac{h}{2Q_1(\xi)} = \frac{1 - \xi}{1 + \xi - \xi^M g(r,\xi)}$$

$$= \frac{1-\xi}{1+\xi}\left(1 + \xi^M \frac{g(r,\xi)}{1+\xi} + \xi^{2M}\frac{g(r,\xi)^2}{(1+\xi)^2} + \cdots\right) = \sum_{n=0}^{\infty} p_n \xi^n$$

where p_n are the stability coefficients. The finite duration of the kernel has no impact on the p_n until $n \geq M$, and it is relatively easy to show that in the first time period after that we have

$$p_n = 2(-1)^n + (-1)^{n+M}(2 - 4r^2 - 8r(1-r)(n-M)),$$
$$M + 2 \leq n \leq 2M - 1.$$

When $r \in (0,1)$, we have $p_n = \mathcal{O}(n) = \mathcal{O}(h^{-1})$, and the scheme is unstable by Definition 3.1. In subsequent time periods (measured in terms of the duration L) it can be shown that the instability gets worse

and $p_n = \mathcal{O}(n^{\lfloor t_n/L \rfloor})$. In the special case when $r = 0$ (or equivalently $L = Mh$) this scheme is stable for this problem, but it may not be possible to satisfy similar integer multiple of h conditions in a more complicated problem, for example, when there are two or more time periods whose ratios are irrational.

Case m = 2, 3. A similar argument can be used to show that these two schemes are unstable for all $r \in [0, 1]$, and that in each case $p_n = \mathcal{O}(n^{\lfloor t_n/L \rfloor})$. Note, however, that the modified cubic spline basis functions described in Section 5 give completely stable results for this kernel.

4.2.3. $K(t) = J_0(\omega t)$, **transform** $\overline{K}(s) = 1/\sqrt{s^2 + \omega^2}$. This is the kernel function that arises when considering TDBIE scattering from the flat surface $\mathbb{R}^2$, where ω can be of the order of $1/h$ (i.e., $h\omega$ is bounded as $h \to 0$, but does not necessarily tend to zero). Its Laplace transform has a branch cut between the values $s = \pm i\omega$, and the Z-transform $Q_m(\xi)$ of the weights is not a rational function. We can still establish stability directly for the impulse response sequence $\{p_n\}$ defined in (3.4) using a change of variable in the Z-transform inversion formula [**15,** eq. 37.7] to get

$$(4.6) \qquad p_n = \frac{e^{nh\sigma}q_0}{2\pi} \int_{-\pi}^{\pi} \frac{e^{iny}}{Q_m(e^{-x-iy})} \, dy,$$

where we have set $\xi = e^{-sh}$ with $s = \sigma + i\eta$ and $\sigma > 0$ and then changed to scaled variables $x = \sigma h$ and $y = \eta h$. This yields the bound

$$(4.7) \qquad |p_n| \leq \frac{e^{\sigma T}}{2\pi} \int_{-\pi}^{\pi} \frac{|q_0| \, dy}{|Q_m(e^{-x-iy})|}$$

when $t_n \leq T$, which holds for any fixed $\sigma > 0$ when the singularities of the integrand are to the left of x. Note that this bound is independent of n, and the scheme is stable at a given frequency ω if the integral term in (4.6) remains bounded as $h \to 0$. This can be demonstrated using the right contour in Figure 3 to calculate $Q_m(e^{-sh})$, but it is more straightforward to work directly with (3.7).

It follows from standard properties of the B-spline basis (4.1) that

$$q_0 = \int_0^h \left(1 - \frac{t}{h}\right)^m J_0(\omega t) \, dt = \frac{m! \, K^{(-m-1)}(h)}{h^m},$$

where functions $K^{(-k)}(t)$ are recursively defined by

$$K^{(0)}(t) = J_0(\omega t), \quad K^{(-k-1)}(t) = \int_0^t K^{(-k)}(t')dt' \quad \text{for } k = 0, 1, \dots .$$

Note that

(4.8) $$K^{(-m-1)}(t) \leq t^{m+1}/(m+1)!$$

for all $t \geq 0$.

Properties of the B-spline basis functions can also be exploited to write (3.7) as

(4.9) $$Q_m(\xi) = \frac{(1-\xi)^{m+1}}{\xi \, h^m} \, \mathcal{Z}\{K^{(-m-1)}\}(\xi) + C_m(\xi),$$

where the correction terms are $C_0 = 0$, $C_1 = 0$,

$$C_2(\xi) = (1 - \xi)\frac{K^{(-3)}(h)}{h^2},$$

$$C_3(\xi) = (1 - \xi)(5 - 3\xi)\frac{K^{(-4)}(h)}{h^3} + \xi(1 - \xi)\frac{K^{(-4)}(2h)}{2\,h^3}.$$

The presence of these terms is because for $m = 0 : 1$ the basis functions are pure translates, while for $m \geq 2$, there are different shaped basis functions at the start. The function $K^{(-k)}$ has Laplace transform

$$\overline{K^{(-k)}}(s) = \frac{1}{s^k\sqrt{s^2 + \omega^2}},$$

and it follows from the Poisson sum formula relating $\mathcal{Z}$ and Laplace transforms that

$$\mathcal{Z}\{K^{(-k)}\}(e^{-sh}) = \frac{1}{h}\sum_{j\in\mathbb{Z}}\frac{1}{s_j^k\sqrt{s_j^2 + \omega^2}} := h^k\sum_{j\in\mathbb{Z}} f_j^{k-1},$$

where $s_j = s + i2\pi j/h$, and we use this expression in (4.9) in order to bound the integral term in (4.7).

When $m = 0$, it is possible to obtain an analytic bound when $\omega \leq \pi/h$, and a careful numerical approximation of the integral (4.7) indicates that the p_n are bounded for ω up to (at least) $20\,\pi/h$. The situation is more complicated for $m = 1 : 3$, and in these cases we give numerical bounds.

Case m $= 0$. From (4.8) and (4.9),

$$\frac{|q_0|}{|Q_0(e^{-x-iy})|} = \frac{1}{|e^{x+iy} - 1| \; \left|\sum_{k\in\mathbb{Z}} f_k^0\right|}$$

and

$$\left|\sum_{k\in\mathbb{Z}} f_k^0\right| = |f_0^0|\left(\left(1 + \sum_{k\in\mathbb{Z}/0} \Re(f_k^0/f_0^0)\right)^2 + \left(\sum_{k\in\mathbb{Z}/0} \Im(f_k^0/f_0^0)\right)^2\right)^{1/2}$$

$$\geq |f_0^0|\left|1 + \sum_{k\in\mathbb{Z}/0} \Re(f_k^0/f_0^0)\right|.$$

It can be shown that

$$1 + \min_y \sum_{k\in\mathbb{Z}/0} \Re\left(f_k^0/f_0^0\right) = 1 + \sum_{k\in\mathbb{Z}/0} \Re\left(f_k^0/f_0^0\right)|_{y=0} > \frac{2}{3},$$

when $0 \leq x \leq 1$, $0 \leq \omega h \leq \pi$ and $|y| \leq \pi$. In this case,

$$\frac{|q_0|}{|Q_0(e^{-x-iy})|} \leq \frac{3\sqrt{x^2 + 2\pi^2}}{2} \frac{\sqrt{x^2 + y^2}}{|e^{x+iy} - 1|} \leq \frac{3\sqrt{x^2 + 2\pi^2}}{2} \frac{\pi e^{-x/2}}{2}$$

using Jordan's inequality. Together with (4.7), this proves that the scheme is stable in the sense of Definition 3.1 for frequency ω in the contiguous interval $0 \leq \omega h \leq \pi$. Numerical evaluation of the right hand side of (4.7) indicates that the bound is

$$|p_n| \leq 1.3\, e^{\sigma T}$$

when h is sufficiently small (so that $x < 0.1$) and $0 \leq \omega h \leq 20\pi$. Further numerical tests computing p_n directly from (3.4) for a finite number of steps $n \leq 2500$ and the same range of values of ωh indicate that $|p_n| \leq 1$, consistent with the estimate above. There is no indication of instability at any value of ωh tested and we speculate that this scheme is stable for all ω.

Case m $= 1$. Finding an explicit bound for the integral in (4.7) is significantly more complicated and perhaps even intractible here, so we only consider its direct numerical evaluation over a range of frequencies and values of $x = h\sigma$ close to 0. However, there is an extra complication because $q_0/Q_1(z)$ has a pole at $z = -1$. This is most obvious when we set $\omega = 0$ and get $q_0/Q_1(z) = (1 - z)/(1 + z)$ from (4.5). When

$\omega \neq 0$, there is no simple formula, but it is still possible to show by direct evaluation of the summation formula for $Q_1(e^{-x-iy})$ that the pole remains when $0 < \omega h < \pi$. The pole renders the bound in (4.7) less useful since

$$|q_0| \int_{-\pi}^{\pi} \frac{dy}{|Q(e^{-x-iy})|} = \mathcal{O}(\log(1/x)) \longrightarrow \infty \quad \text{as } x \to 0$$

(where $x = h\sigma$), and hence $|p_n| \leq (C_0 + C_1 \log(1/h))e^{\sigma T}$ as $h \to 0$, which does not satisfy the stability requirement of Definition 3.1. Fortunately, the singularity can be removed by writing

$$\frac{q_0}{Q_1(\xi)} = \frac{a}{(1+\xi)} + \Delta P(\xi), \quad \text{where } a = \lim_{\xi \to -1} \frac{q_0(1+\xi)}{Q_1(\xi)}$$

so that $\Delta P(\xi)$ is bounded as $\xi \to -1$. The sequence $\{p_n\}$ can then be written as $p_n = a\,(-1)^n + \Delta p_n$ where Δp_n is bounded in the same way as (4.7):

$$(4.10) \qquad |\Delta p_n| \leq \frac{1}{2\pi} \int_{-\pi}^{\pi} |\Delta P(x+iy)|\, dy.$$

Numerical evaluation of the integral over frequencies $0 \leq \omega h < \pi$ indicates that $|\Delta p_n| \leq 1.1$ and $0 < a \leq 2$ for $nh \leq T$ and $0 < x \leq 1/10$. Combining this with direct evaluation of (4.7) when $\omega h \in [\pi, 20\pi]$ and there is not a pole indicates that

$$|p_n| \leq Ce^{\sigma T} \quad \text{where } C = \begin{cases} 3.1, & \omega h \in [0, \pi) \\ 1.1, & \omega h \in [\pi, 20\pi] \end{cases}$$

for $nh \leq T$ and $0 < x \leq 1/10$ satisfying the stability Definition 3.1. Further numerical tests computing p_n directly from (3.4) for a finite number of steps $n \leq 2500$ and the same range of values of ωh indicate that $|p_n| \leq 2$ for $\omega h \in [0, 0.7\pi)$ and $|p_n| \leq 1$ for $\omega h \in [0.7\pi, 20\pi]$, consistent with the estimate above. Again, we speculate that this scheme is stable for all ω.

Case $m = 2$. The function $q_0/Q_2(\xi)$ appears to have two poles on the unit circle when $\omega h \in [0, L)$ where $L \approx 2.55$, symmetrically located at $\xi = e^{\pm i\mu(\omega h)}$. In the simple case $\omega = 0$, (4.5) gives $Q_2(\xi) = q_0\,(1+\xi+\xi^2)/(1-\xi)$, and so $\mu(0) = 2\pi/3$. Numerical evidence indicates that $\mu(\omega h) > \omega h$ and that μ increases until the two poles meet where $\mu(L) = \pi$. At that point stability in the sense of Definition 3.1

breaks down since there does not appear to be any compensating factor in the numerator to reduce the order of this double singularity.

We locate the poles numerically and remove them from the integrand $q_0/Q_2(\xi)$ in a similar way to the previous case. The simplest form that captures the main features of the behavior is

$$\frac{q_0}{Q_2(\xi)} = \frac{a(1-\xi)}{\xi^2 - 2\xi \cos \mu + 1} + \Delta P(\xi),$$

so that by direct inversion of the Z transform,

$$p_n = a(\cos(n\mu) - \sin(n\mu)\tan(\mu/2)) + \Delta p_n.$$

For $0 \le \omega h < L \approx 2.55$, we find that $0 < a \le 1$, and from (4.10) that $|\Delta p_n| \le 0.8$, giving

$$|p_n| \le 0.8 + \sec(\mu(\omega h)/2)$$

for $nh \le T$ when $0 < x \le 1/10$. This satisfies Definition 3.1 since $2\pi/3 \le \mu(\omega h) < \pi$, but since $\sec(\mu/2) \to \infty$ as $\mu \to \pi$, the possibility for instability is clear. Further numerical tests computing p_n directly from (3.4) for a finite number of steps show very close and consistent agreement with this bound on $|p_n|$, with instability appearing as predicted at $\omega h = L \approx 2.55$, i.e., there is a contiguous interval of stability $\omega h \in [0, L)$ with $L \approx 2.55$.

Case m = 3. Not surprisingly, this case is more complicated still. When $\omega = 0$, the three poles of $q_0/Q_3(\xi)$ are on the unit circle at $\xi = -1, e^{\pm i\pi/2}$. However, when $\omega h > 0$ increases, the real-valued pole at $\xi = -1$ moves (harmlessly) outside the unit circle while the other complex conjugate pair moves inside causing instability. Numerical tests computing p_n directly from (3.4) for fixed values of ωh show behavior consistent with this: we see apparent stability for larger values of h which disappears as $h \to 0$, i.e., this scheme is stable only when ω is fixed (so that $\omega h \to 0$).

Similar results can be proved for the (more straightforward) oscillatory kernel $K(t) = \cos \omega t$, as summarized below.

- **m = 0**. The scheme is stable at any frequency ω for which $\omega h \in [0, \pi)$.
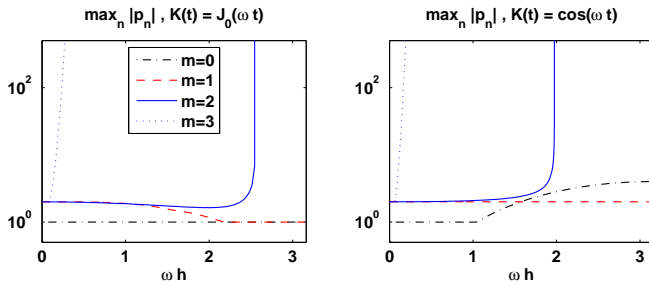
FIGURE 4.   Plots of $\max \{|p_n| : 0 \leq n \leq 2500\}$ against ωh for the B-spline schemes with $m = 0 : 3$ applied to the highly oscillatory kernels $K(t) = J_0(\omega t)$ (left plot) and $K(t) = \cos \omega t$ (right plot). (See text for more details.)

- **$m = 1$.** The scheme is stable at any frequency ω for which $\omega h \in [0, 2\pi)$.
- **$m = 2$.** The scheme is stable at any frequency ω for which $\omega h \in [0, \theta)$, where $\theta = 1.9747\ldots$.
- **$m = 3$.** There is no $\mathcal{O}(1)$ interval of stability for ωh, but the scheme is stable for bounded ω.

The stability results for highly oscillatory kernels are illustrated in Figure 4. The plots show $\max_n |p_n|$ for $n = 0 : 2500$ for the B-spline schemes with $m = 0 : 3$ applied to the kernels $K(t) = J_0(\omega t)$ (left plot) and $K(t) = \cos \omega t$ (right plot). Over the range $\omega \in [0, \pi/h]$ shown, the general stability behavior for these two kernels is similar. In particular, the left plot illustrates the stability when $m = 0, 1$, while scheme $m = 2$ is stable for $\omega h \in [0, L]$ with $L \approx 2.55$. On the right plot, scheme $m = 0$ is stable except at $\omega h = \pi$, scheme $m = 1$ is stable and $m = 2$ scheme is stable for $\omega h \in [0, L]$ with $L \approx 1.97$. On both plots the $m = 3$ scheme is clearly unstable when $\omega = \mathcal{O}(1/h)$.

4.3. Convergence results for (3.3). Formal convergence of a method when applied to a smooth VIE problem is certainly a necessary condition for it to behave well (for VIEs or TDBIEs), and we now prove that the collocation spline approximation (3.3) with B-spline basis functions (4.1) converges to the solution u of (1.2) for general smooth a and K. The analysis proceeds by considering case $K \equiv 1$ and then using Taylor

expansion to show that the same result also holds for smooth K with $K(0) = 1$ when h is small enough (see, e.g., [6]). Thus, it does not apply to the important case of an oscillatory kernel where the oscillation frequency $\omega = \mathcal{O}(1/h)$, whose stability was analyzed above for the Bessel function and cosine kernels.

When $m = 0$, the approximation (3.2) is the same as using piecewise constant collocation (at the interval endpoints), and this has been fully analyzed (see, e.g., [6] for details). Here we assume that $m \geq 1$ (note that this includes the well-known case of piecewise linear approximations of (1.2)), and show that convergence is always second order, no matter how high the polynomial degree, because quasi-interpolation by the Schoenberg B-spline operator is at most $\mathcal{O}(h^2)$ [14]. This is in marked contrast to discontinuous polynomial collocation or Galerkin approximations of (1.2) which converge at optimal order [6, 7, 8]. However, a simple modification of the B-spline basis near $t = 0$ can give higher order stable approximations of (1.2), as illustrated when $m = 3$ in Section 5.

The *approximation error* $e_n(t)$ for $n > 0$, $t \geq 0$ is

$$(4.11) \qquad e_n(t) = u(t_n - t) - \sum_{j=0}^{n} v_{n-j} b_{j-m}^m(t),$$

where the coefficients v_j satisfy

$$(4.12) \qquad a(t_n) = \sum_{j=0}^{n} q_j v_{n-j}$$

for weights q_j as defined in (4.4). Note that $v_0 = 0$ (because $a(0) = 0$), so the sums above can be taken from $j = 0$ to $n-1$, and it then follows from Property P1 that $e_n(t) = 0$ for $t \geq t_n$ and each weight can be written as $q_j = \int_0^{t_n} K(t) b_{j-m}^m(t)\, dt$. Hence, multiplying (4.11) by $K(t)$ and integrating gives

$$\int_0^{t_n} K(t) e_n(t)\, dt = \int_0^{t_n} K(t)\, u(t_n - t)\, dt - \sum_{j=0}^{n-1} q_j v_{n-j} = 0,$$

by (1.2) and (4.12), i.e., e_n is orthogonal to K on $(0, t_n)$. The formal convergence result is as follows.
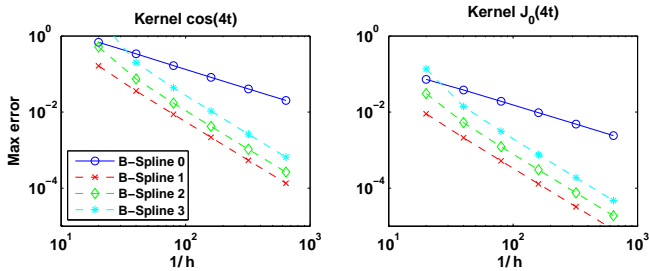
FIGURE 5. Convergence results for the approximation of (1.2) for two smooth kernel functions with maximum time $T = 10$ and $a(t) = t^6 \exp(-50(t-1/2)^2)$. Convergence rates of $\mathcal{O}(h^2)$ for splines of degree $m \geq 1$ and $\mathcal{O}(h)$ for $m = 0$ are clear. Stability results for the highly oscillatory kernels $\cos \omega t$ and $J_0(\omega t)$ where the frequency ω can be $\mathcal{O}(1/h)$ are given in subsection 4.2 and Figure 4.

Theorem 4.1. *Suppose that $m \geq 1$ and the conditions (1.5) and (2.1) hold for $d \geq 4$. Then*

$$(4.13) \qquad\qquad |e_n(t)| \leq C\, h^2$$

for $t \in [t_m, T]$, for some C independent of n and h. If $m = 1$, then (4.13) holds for $t \in [0, T]$.

Remarks.

- The $m = 1$ case has been fully analyzed [6] and is only included for completeness.
- The restriction to second order convergence for $m > 1$ is a fundamental aspect of quasi-interpolation by classical B-splines and not an artifact of the proof, and is illustrated in Figure 5 when (2.1) holds with $d = 4$.
- Equation (4.13) trivially holds for $t \geq t_n$ (because $e_n(t) = 0$), and so it is enough to prove the result for $t \in [t_m, t_n)$ when $m > 1$, where $n \leq T/h$.

Proof. We first express $e_n(t)$ in terms of coefficients $\varepsilon_k := u(t_{k+(m-1)/2})$ $- v_k$. Substituting the quasi-interpolation result (4.2) with $f(t) =$

$u(t_n - t)$ in the definition (4.11) of $e_n(t)$ gives

$$e_n(t) = \sum_{j=m}^{n} \varepsilon_{n-j} b^m_{j-m}(t) + \sum_{j=n+1}^{n+m} u(t_n - t^m_{j-m}) \, b^m_{j-m}(t) + \mathcal{O}(h^2),$$

where we have used $b^m_{j-m}(t) = 0$ for $j < m$ and $j > n + m$. It follows from assumptions (1.5) and (2.1) that $u(ch) = \mathcal{O}(h^d)$ for any constant c. This implies that the second sum term in the previous equation is $\mathcal{O}(h^d)$, and hence yields

$$e_n(t) = \sum_{j=m}^{n} \varepsilon_{n-j} \, b^m_{j-m}(t) + \mathcal{O}(h^2)$$

for $t \in [t_m, t_n)$ with $t_n \leq T$. Because there are at most $m + 1$ nonzero terms in this sum for any t, it is sufficient to show that there exists a constant C independent of h such that

(4.14) $|\varepsilon_j| \leq Ch^2$ for all $j \leq T/h$.

To prove (4.14), note that it follows from (4.12) that

$$\sum_{j=0}^{n} q_j \, v_{n-j} = \int_0^{t_n} K(t) \, u(t_n - t) \, dt,$$

and so

(4.15) $$\sum_{j=0}^{n} \frac{q_j}{h} \varepsilon_{n-j} = \sum_{j=0}^{n} \frac{q_j}{h} u(t_{n-j+(m-1)/2})$$

$$- \frac{1}{h} \int_0^{t_n} K(t) \, u(t_n - t) \, dt := R_n.$$

If h is sufficiently small, then expanding $K(t)$ and using P4 gives
(4.16)
$$\frac{q_j}{h} = \begin{cases} \frac{j+1}{m+1} + h \, K'(0) \frac{(j+1)^2(j+2)}{2(m+1)(m+2)} + \mathcal{O}(h^2) & \text{for } j = 0 : m - 1, \\ K(t_{j-m}) + \frac{1}{2} h(m+1) \, K'(t_{j-m}) + \mathcal{O}(h^2) & \text{if } j \geq m. \end{cases}$$

It then follows from the quasi-interpolation result (4.3) with $p = 3$, when $n \geq m$, that

$$hR_n = \sum_{\ell=0}^{n-1} \sum_{k=2}^{3} \eta^k_\ell u^{(k)}(t_{n-\ell}) + \mathcal{O}(h^4) \quad \text{for}$$

$$\eta_\ell^k = \frac{(-1)^{k+1}}{k!} \int_{t_\ell}^{t_{\ell+1}} K(t) \left\{ (t - t_\ell)^k - \sum_{j=\ell}^{\ell+m} (t_{j-m} - t_\ell)^k b_{j-m}^m(t) \right\} dt.$$

It is then straightforward to show $R_{n+1} - 2R_n + R_{n-1} = \mathcal{O}(h^3)$ and, after some manipulation using (4.16), the second central difference of (4.15) can be written as
(4.17)

$$(1 + h\mu_o)\varepsilon_{n+m+1} = \varepsilon_n + h\sum_{\ell=0}^{m} \mu_{\ell+1}\varepsilon_{n-\ell+m} + h^2 \sum_{\ell=m+1}^{n} \mu_{\ell+1}\varepsilon_{n-\ell+m} + \gamma_n,$$

where $\gamma_n = \mathcal{O}(h^3)$ and all the μ_ℓ are bounded. This can be written as a one-step recurrence for the vector $\underline{\delta}^n \in \mathbb{R}^{m+1}$ with components $\delta_j^n \equiv \varepsilon_{n+j}$ for $j = 0 : m$. The recurrence is $\delta_j^{n+1} = \delta_{j+1}^n$ for $j = 0 : m-1$ with δ_m^{n+1} given by (4.17), which gives the matrix-vector system

$$(4.18) \qquad \underline{\delta}^{n+1} = (M + hW_0)\underline{\delta}^n + h^2 \sum_{\ell=0}^{n-1-m} W_{n-\ell}\underline{\delta}^{m+\ell} + \gamma_n \underline{e}^m$$

where $\underline{e}^m = (0, \ldots, 0, 1)^T$, each matrix W_ℓ is bounded and $M \in \mathbb{R}^{(m+1)\times(m+1)}$ is the circulant matrix whose only nonzero components are $M_{m,0} = M_{j,j+1} = 1$ for $j = 0 : m - 1$. The eigenvalues of M are the $(m+1)$th roots of unity, and are hence distinct. Following Brunner [5] we note that M belongs to Ortega's [**34**, subsection 1.3] Class M, and so there is a vector norm $\|\cdot\|_*$ on $\mathbb{R}^{m+1}$ for which the induced matrix norm satisfies $\|M\|_* = \rho(M) = 1$. Taking this norm of (4.18) then implies that there is a constant C such that

$$\|\underline{\delta}^{n+1}\|_* \leq (1 + Ch)\|\underline{\delta}^n\|_* + Ch^2 \sum_{\ell=0}^{n+1-m} \|\underline{\delta}^{m+\ell}\|_* + Ch^3$$

and the top bound of (4.14) gives $\|\underline{\delta}^0\|_* \leq Ch^d$. Standard arguments can then be used to show that $\|\underline{\delta}^n\|_* \leq \nu_n$ where $\nu_0 = Ch^d$ and

$$(4.19) \qquad \nu_{n+1} = (1 + Ch)\nu_n + Ch^2 \sum_{\ell=0}^{n} \nu_\ell + Ch^3 \quad \text{for } n \geq 0.$$

This has the solution $\nu_n = A_+\lambda_+^n + A_-\lambda_-^n$ where $\lambda_\pm = 1 + \mathcal{O}(h)$ and $A_\pm = \mathcal{O}(h^2)$. Hence, $\nu_n \leq C_1 h^2 e^{C_2 T}$ for $n \leq T/h$, which concludes the proof of (4.14) and hence (4.13). $\qquad \square$

5. Modified cubic spline basis functions for (1.2). The results of the previous section illustrate that the convolution spline framework can be used to derive new VIE approximations and prove their stability in cases not covered by standard convergence analysis (such as discontinuous or highly oscillatory kernels), but the restriction to second order convergence for the B-spline basis (4.1) is not competitive with RK-based CQ methods [**2, 3, 4**]. We now show how a slight modification of the $m = 3$ B-spline basis near $t = 0$ can yield methods which are more accurate and have better stability properties than (4.1).

5.1. Derivation. It is simpler to define the modified basis functions in terms of B-splines centred at zero, and we set $B(t) = b^3(t + 2)$, so $\text{supp}(B) = (-2, 2)$. For $j \geq 3$ the basis functions are $\phi_j(t) = B(t - j)$, and we choose ϕ_j for $j = 0 : 2$ to satisfy the parabolic runout conditions at $t = 0$, namely,

$$\phi_0(t) = B(t) + 3\,B(t + 1),$$
$$\phi_1(t) = B(t - 1) - 3\,B(t + 1),$$
$$\phi_2(t) = B(t - 2) + B(t + 1).$$

This means that

$$(5.1) \qquad \sum_{j=-1}^{\infty} j^r \left(\phi_j(t) - B(t - j)\right) = 0 \quad \text{for } t \in [0, \infty) \text{ for } r = 0 : 2,$$

where we set $\phi_{-1}(t) \equiv 0$, and in particular it ensures that quasi-interpolation in terms of $\{\phi_j\}_{j=0}^{\infty}$ is linearity-preserving on $[0, \infty)$. Weights q_j for the VIE (1.2) are given in terms of these basis functions by (2.10), and the approximation at $t = t_n$ is

$$(5.2) \qquad U_n(t_n - t) = \sum_{j=0}^{n} v_{n-j}\phi_j(t/h),$$

where the v_j coefficients are given by (3.3). The individual coefficients can be directly obtained from $U_n(t_n - t)$ by introducing dual basis functions $\phi_k^*(t)$ such that

$$\int_0^{\infty} \phi_j(t)\,\phi_k^*(t)\,dt = \delta_{j,k}.$$

There are many ways in which a suitable dual basis can be chosen, and one possibility is to use continuous piecewise cubic functions on $[0, \infty)$ defined with respect to knots in $\mathbb{N}$. For $k \geq 3$, we set $\phi_k^*(t) = \phi^*(t - k)$ where ϕ^* is the even continuous piecewise cubic function on $[-2, 2]$ which is zero at ± 2 and is C^1 at the interior knots ± 1, 0 and satisfies

$$\int_{-2}^{2} \phi^*(t - \ell)\, B(t)\, dt = \delta_{0,\ell} \quad \text{for } \ell = 0 : 3,$$

and it is also possible to find suitable continuous piecewise cubics ϕ_k^* with support in $[0, k + 2)$ for $k = 0 : 2$. Calculating these dual basis functions in an algebraic manipulation package is straightforward, although their coefficients are messy and we omit their details. Once the ϕ_k^* have been obtained, it can be shown by Taylor expanding that for any sufficiently smooth function f,

$$(5.3) \quad \int_{\max(0, k-2)}^{k+2} f(t_n - hs)\, \phi_k^*(s)\, ds = f(t_{n-k}) - \frac{h^2}{6}\, f''(t_{n-k}) + \mathcal{O}(h^4).$$

Multiplying (5.2) by $\phi_k^*(t/h)$ and integrating over $[0, \infty)$ gives

$$v_{n-k} = \int_{\max(0, k-2)}^{k+2} U_n(t_n - hs)\, \phi_k^*(s)\, ds$$

and we now use this representation and (5.3) in order to obtain the best approximation of the solution u of (1.2) in terms of the basis functions ϕ_j when (1.5) holds with $d = 4$. Specifically, we set

$$(5.4) \qquad u(t_n - t) = \sum_{j=0}^{n} u_{n-j}\, \phi_j(t/h) + \widetilde{R}_n(t),$$

where
(5.5)
$$u_{n-j} := \int_{\max(0, j-2)}^{j+2} u(t_n - hs)\, \phi_j^*(s)\, ds = u(t_{n-j}) - \frac{h^2}{6}\, u''(t_{n-j}) + \mathcal{O}(h^4).$$

We show that this scheme is fourth order accurate, and discuss its stability properties for non-smooth kernels.

5.2. Convergence. It follows from (5.4)–(5.5) that the approximation error $e_n(t) := u(t_n - t) - U_n(t_n - t)$ for this scheme is

$$e_n(t) = \sum_{j=0}^{n} \varepsilon_{n-j}\, \phi_j(t/h) + \widetilde{R}_n(t)$$

where $\varepsilon_k = u_k - v_k$. We now show that modifying the basis functions near $t = 0$ as described above improves the scheme's accuracy from second to fourth order.

Theorem 5.1. *Suppose that the conditions* (1.5) *and* (2.1) *hold for* $d \geq 6$. *Then there exists a constant C independent of n and h such that, if $t_n \leq T$, the* VIE *approximation error satisfies*

(5.6) $$|e_n(t)| \leq C\, h^4$$

for $t \in [t_1, t_n]$.

Proof. It is straightforward to verify that, if $s \in [0, 1)$,

$$\widetilde{R}_n(t_k + hs) = u(t_{n-k} - hs) - \sum_{\ell=-1}^{2} u_{n-k-\ell}\phi_{k+l}(k+s),$$

where ϕ_{-1} is taken to be zero, and hence it follows from (5.1), (5.5) and standard B-spline properties that

$$\widetilde{R}_n(t_k + hs) = \begin{cases} h^3(1-s)^3\, u'''(t_n)/6 + \mathcal{O}(h^4) & \text{when } k = 0 \\ \mathcal{O}(h^4) & \text{when } k \geq 1. \end{cases}$$

It is thus sufficient to show that each $\varepsilon_k = \mathcal{O}(h^4)$ (because at most four basis functions are nonzero for any t). The proof follows that of Theorem 4.1, and the expression analogous to (4.15) is

$$\sum_{j=0}^{n-1} \frac{q_j}{h}\, \varepsilon_{n-j} = -\sum_{k=0}^{n} \int_0^1 K(t_k + hs)\, \widetilde{R}_n(t_k + hs)\, ds + \mathcal{O}(h^5).$$

Taking the second central difference, using the fact that when $K \equiv 1$, the scheme coefficients are
(5.7)
$$q_0 = 5h/8, \quad q_1 = 5h/6, \quad q_2 = 25h/24, \quad \text{and} \quad q_j = h \text{ for } j \geq 3$$

gives an expression like (4.18) with $m = 3$ where the bottom row of the matrix M is now $[-1, 6, 0, 10]/15$. The eigenvalues of M are all distinct, its spectral radius is $\rho(M) = 1$, and this again yields a bound ν_n which satisfies a difference scheme like (4.19) whose final term is $C h^5$. This gives an $\mathcal{O}(h^4)$ bound for each $|\varepsilon_k|$ with $t_k \leq T$, and (5.6) follows. $\qquad\square$

5.3. Stability for discontinuous and highly oscillatory kernels.
We first consider the discontinuous kernel introduced in subsection 4.2. The duration $L = (M + r)h$ is fixed independent of h such that integer $M \geq 5$ and $r \in [0, 1)$. In this case the q_j are given by (5.7) for $j = 0 : M - 2$, the coefficients q_j for $j = M - 1 : M + 2$ are polynomial in r and satisfy

$$q_{M-2} = h \geq q_{M-1} \geq q_M \geq q_{M+1} \geq q_{M+2} \geq 0,$$

and $q_j = 0$ for $j \geq M + 3$.

The stability proof follows that of [**13**, subsection 3.1.3]; forward differencing (3.4) gives

$$15\,p_n + 5\,p_{n-1} + 5\,p_{n-2} - p_{n-3} + 24 \sum_{j=M-1}^{M+3} \frac{(q_j - q_{j-1})}{h}\,p_{n-j} = 0 \text{ for } n \geq 2,$$

where the first stability factors are $p_0 = 1$, $p_1 = -q_1/q_0 = -4/3$, and we set $p_j = 0$ for $j < 0$. Similar manipulations to those in the previous subsection then give

$$|p_n| \leq \frac{11}{15}\, Z_{n-1} + \frac{8}{5}\, Z_{n-(M-1)} \quad \text{for } n \geq 2,$$

where now $Z_k = \max_{j \leq k} |p_j|$. It then follows from similar arguments to those used in [**13**, subsections 3.1.3] that, if $n \geq M - 1$, then

$$Z_n \leq \frac{11}{15}\, Z_{n-1} + \frac{8}{5}\, Z_{n-(M-1)} \leq \frac{11}{15}\, Z_n + \frac{8}{5}\, Z_{n-(M-1)},$$

i.e., $Z_n \leq 6\, Z_{n-(M-1)}$, and $|p_n| \leq Z_n = 4/3$ for $n = 1 : M - 2$. In combination, these give the stability bound

$$|p_n| \leq Z_n \leq C\, 6^{n/(M-1)} \leq C\, 6^{(T+1)/L}$$

for all $n \leq T/h$ when h is sufficiently small, and so the stability coefficients are bounded independently of h as required by Definition 3.1.

Note that this bound is very pessimistic, and in practice the factor is about $1.5^{T/L}$.

This scheme is also stable when applied to the oscillatory kernels $J_0(\omega t)$ and $\cos(\omega t)$ examined in subsection 4.2. The analysis is much simpler to carry out for this scheme, since there is no problem with poles of $1/Q(\xi)$ on or near the unit circle $|\xi| = 1$. We find that

$$|p_n| \leq Ce^{\sigma T} \quad \text{where } C = \begin{cases} 2.2 & \text{for } K(t) = \cos(\omega t), \\ 1.5 & \text{for } K(t) = J_0(\omega t), \end{cases}$$

for all $\omega h \in [0, 20\pi]$ and beyond. This is verified in tests computing p_n directly from (3.4) for a finite number of steps $n \leq 2500$ and the same range of values of ωh. They indicate that $|p_n| \leq 1.82$ (for $\cos(\omega t)$) and $|p_n| \leq 4/3$ (for $J_0(\omega t)$), consistent with the estimate above.
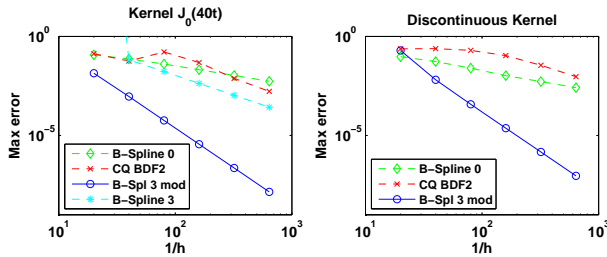

FIGURE 6. Convergence results for the approximation of (1.2) with maximum time $T = 10$ and $a(t) = t^6 \exp(-50(t - 1/2)^2)$ (see text for details). The stability and $\mathcal{O}(h^4)$ convergence rate of modified B-spline 3 is clear for both problems.

5.4. Numerical results. Numerical comparisons of the new modified cubic B-spline approximation for (1.2) are compared with the CQ BDF2 method and with the convolution B-splines with $m = 0, 3$ from Section 4 in Figure 6 when a satisfies (2.1) with $d = 4$. The convergence rates for a smooth kernel (left subplot) are as expected: CQ BDF2 has rate $\mathcal{O}(h^2)$; B-splines 0 and 3 have rates $\mathcal{O}(h)$ and $\mathcal{O}(h^2)$; and the modified B-spline 3 has rate $\mathcal{O}(h^4)$. The discontinuous kernel problem (right subplot) has the same convergence rates, apart from the isogeometric $m = 3$ approximation which was shown to be unstable in subsection 4.2, and is not illustrated.

6. Convolution splines for TDBIEs. The results shown here are obtained by approximating the solution of the TDBIE (1.1) in space by piecewise constant basis functions on a generally irregular triangular grid, and in time by convolution splines as

$$u(\vec{x}, t_n - t') \approx \sum_{j=0}^{n} \sum_{k=1}^{M} u_k^{n-j} \phi_j(t'/h)\, \eta_k(\vec{x}),$$

where the ϕ_j are the modified cubic B-splines from subsection 5.1,

$$\eta_k(\vec{x}) = \begin{cases} 1 & \text{for } \vec{x} \in \Gamma_k \\ 0 & \text{otherwise,} \end{cases}$$

and Γ_k is the kth triangle on the surface Γ. The spatial Galerkin formulation of the problem gives the time-marching scheme (1.3) with

$$\mathsf{Q}_{j,k}^m = \iint_{\Gamma_j \times \Gamma_k} \frac{\phi_m(|\vec{x} - \vec{y}|/h)}{|\vec{x} - \vec{y}|}\, d\vec{x}\, d\vec{y}, \quad \text{and} \quad a_j^n = \int_{\Gamma_j} a(\vec{x}, t^n)\, d\vec{x}.$$

The matrices Q^m are symmetric, and calculating each component involves a four dimensional integral. The off-diagonal components and the components a_j^n have smooth integrands and are approximated by a composite triangular quadrature with 16 sub-triangles, each of which is fourth order with six quadrature points. Each diagonal element of the Q^m has a singular integrand and is first converted into smooth subintegrals using a Duffy-type transformation and then approximated by the same quadrature rule as the rest of the calculation.

The piecewise constant spatial approximation is globally first order accurate (i.e., $\mathcal{O}(\Delta x)$), but there is local (second order) superconvergence at the element midpoints, and this is exploited in the figures below. In particular, $\|\cdot\|_\infty$ is the discrete L_∞ norm measured at element midpoints. Similar results are obtained when piecewise linear spatial basis functions are used (this is globally second order). A more accurate spatial approximation could potentially be used (to take advantage of the fourth order accuracy in time), along with higher order quadrature.

Figure 7 shows results for (1.1) when Γ is a flat plate and a sphere, both with incident field $a(\vec{x}, t) = a_0(t + t_0 - |\vec{x}|)/|\vec{x}|$, where $a_0(t) = t^4 \exp(-20(t - 1/2)^2)$ for $t > 0$. In these two tests the mesh ratio is chosen to be $h/\Delta x = 1/2$, where Δx is the size of a typical space
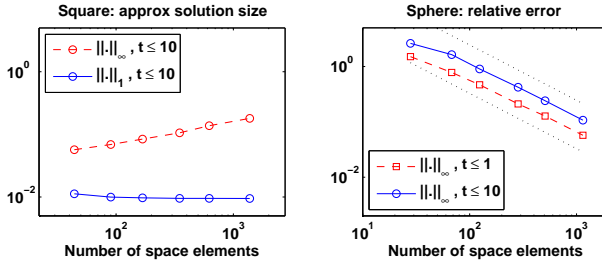
FIGURE 7. Solution plots for the TDBIE (1.1) when the scattering surface Γ is a unit square plate (left plot) and a unit sphere (right plot). See text for details of the space and time approximations used.
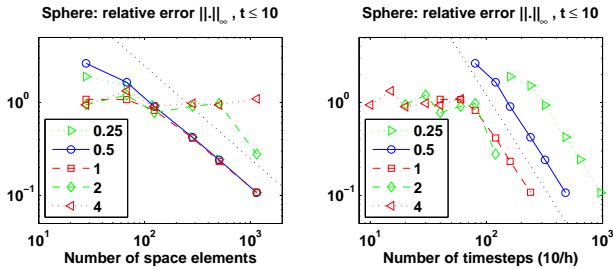

FIGURE 8. Solution plots for the TDBIE (1.1) for mesh ratios $h/\Delta x$ ranging from 0.25 to 4 when the scattering surface Γ is a unit sphere. The dotted line indicates second order convergence. See text for details of the space and time approximations used.

mesh element. The left-hand graph shows the size (and hence stability) of the approximate solution on a unit square plate. The growth in the L_∞ norm is due to a corner singularity in the exact solution [25] while the maximum of the 1-norm is well-behaved as the mesh is refined. The right-hand plot shows the maximum relative error (i.e., the error normalized by the maximum size of the solution) for scattering from a unit sphere–an exact solution for this problem is given in [37]. The dotted lines show a second order convergence slope, and this is the best which can be expected from the spatial approximation, despite the higher order accuracy of the temporal approximation.

Figure 8 demonstrates the impact of changing the mesh ratio $h/\Delta x$ in the sphere scattering example described above. The left plot shows the maximum relative error in the solution against the number of space elements, and the right plot shows the dependence of this error on h. As one would expect for a scheme with higher order accuracy in time than space, the time error decreases faster than the space error when the mesh is refined with fixed mesh ratio, and the space error eventually dominates. This is clear on the left plot for ratios $h/\Delta x = 0.25$, 0.5 and 1. For the larger mesh ratios the time step size is simply too big to resolve the input function accurately, and the asymptotic convergence regime has not yet been reached. Increasing the mesh ratio decreases the number of time steps (and hence matrices Q^m) used but increases the number of non-zero entries in each matrix. However, the net result is a decrease in the computational cost for both the time marching calculation and the computation of the matrices Q^m.
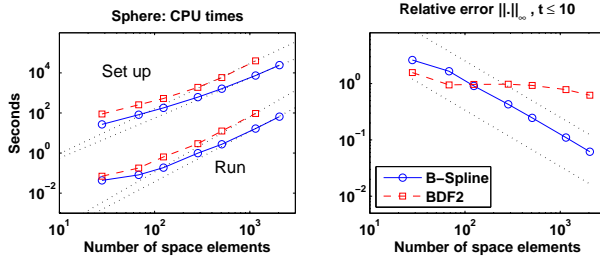

FIGURE 9. Solution plots for the TDBIE (1.1) with time approximation given by convolution cubic splines (blue solid) and CQ based on BDF2 (red dashed) when Γ is a unit sphere. **Left plot:** shows the CPU time in seconds for computing the system matrices (set up) and the algorithm run time–the dotted lines represent the asymptotic computational complexity $\mathcal{O}(N^p)$ for each approach described in the text. **Right plot:** shows the relative error vs N_S for each method, and the dotted lines indicate second order convergence.

The final set of results compares the performance of convolution cubic splines for time-stepping TDBIEs with that of CQ based on BDF2. The *set-up time* for each method is proportional to the number of non-zero entries in the Q^m matrices of (1.3) (with sufficiently small entries in the CQ case ignored). For convolution spline (and space-time Galerkin) methods, this is $\mathcal{O}(N^4)$ when $h \approx \Delta x = 1/N$. The support

of the CQ basis functions grows with m, as illustrated in Figure 2 (see also [**23**]), and the set-up cost for this method is $\mathcal{O}(N^{4.5})$. As described in subsection 1.1, the *run time* for the basic convolution spline schemes (i.e., without using a plane-wave or other fast method to speed it up) is $\mathcal{O}(N^5)$, and for the basic CQ approach it is $\mathcal{O}(N^{5.5})$. The left-hand plot of Figure 9 shows a graph of CPU time against the number of space elements, and the dotted lines in each case show the asymptotic computational complexity $\mathcal{O}(N^p)$ as tabulated below. Note that, although for each method the run time is clearly growing faster with $N_S \approx N^2$ than the set up time, the set-up time dominates for problems of moderate size.

Method	Setup	Run
spline	$\mathcal{O}(N^4)$	$\mathcal{O}(N^5)$
CQ	$\mathcal{O}(N^{4.5})$	$\mathcal{O}(N^{5.5})$

TABLE 3. Computational complexity $\mathcal{O}(N^p)$ of the set up and run times for algorithm (1.3) with time approximation given by convolution spline and CQ, where $h \approx \Delta x = 1/N$.
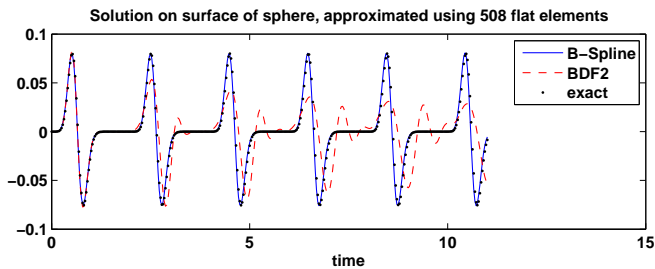

FIGURE 10. Approximate solution u of (1.1) plotted against time when Γ is a unit sphere. The exact solution is independent of $\vec{x}$ and is shown as black dots, and the approximate solution is calculated using convolution spline (blue solid) and CQ based on BDF2 (red dashed).

The right-hand plot of Figure 9 shows the approximation error for the two schemes, with dotted lines of slope $\mathcal{O}(\Delta x^2)$. The far superior accuracy of the convolution spline approximation is clear, and the poor

performance of the BDF2 CQ method is because it is highly damped–
although it is second order convergent, the mesh has to be very fine
for this to be apparent over a long time calculation. This is further
illustrated in Figure 10, which shows the potential u calculated on the
surface of the sphere vs time when $N_S = 508$. The convolution spline
approximation matches the exact solution (which is independent of $\vec{x}$,
see [37]) extremely well.

7. Conclusions. We have derived a new framework for time-stepping
approximations of the TDBIE (1.1). The system matrices Q^m of the
resulting scheme (1.3) have the same degree of sparsity as for a space-
time Galerkin approximation but are much more straightforward to
calculate, especially when higher order (smoother) B-splines are used.
The method is constructed as an approximation scheme for the VIE
(1.2), and key properties are its backward time aspect (2.9) that the
basis functions have compact support and are (mainly) translates, and
they satisfy the sum to unity condition (2.12).

These properties permit a full stability analysis for VIEs with kernels
which capture some of the important properties of TDBIE problems,
as illustrated for B-spline basis functions in subsections 4.2 and 5.3. In
particular, the analysis gives a stability bound for the p_n coefficients
for the Bessel function kernel (1.4) when $\omega \approx 1/h$. This means that
the convergence proof in [11] for the TDBIE (1.1) on $\Gamma = \mathbb{R}^2$ could be
applied to an approximation which is a Fourier interpolant in space and
a convolution spline in time, without the need to impose an additional
(essentially uncheckable) stability assumption. The modified cubic
convolution spline approximation of Section 5 is fourth order accurate
and gives a very stable approximation for discontinuous and highly
oscillatory VIE kernels. The TDBIE numerical test results indicate
that the scheme is very stable and performs well.

There is current interest in TDBIE time-stepping methods which
can use variable time-steps, see e.g., [27, 28] for convolution quad-
rature methods and [19] for space and time adaptation in the full
space-time Galerkin method for scattering problems in 2D space. Be-
cause our TDBIE time-stepping method is based on B-splines (whose
key approximation properties are retained for a non-uniform knot dis-
tribution) and standard piecewise polynomials in space, the various
strategies described in [19] for space and time adaptation could be

applied. However, using variable time-stepping in any TDBIE approximation algorithm imposes an overhead because it essentially involves recalculating the Q^m matrices of (1.3) at every time step, and this is extremely expensive, as illustrated in the left-hand plot of Figure 9.

We note that there are also other choices of basis functions which seem to give stable approximations of (1.2) and (1.1) when used in the same convolution framework. Non-polynomial temporal basis functions ϕ_j are introduced in [13]; they are translates for $j \geq 2$, and for $j = 0 : 1$ they are defined as described in [40] for radial basis function (RBF) multi-quadrics in order to ensure that quasi-interpolation in terms of $\{\phi_j\}_{j=0}^{\infty}$ is linearity-preserving. They also work well as a temporal approximation of the TDBIE (1.1) but, because the basis functions are global, the system matrices need to be sparsified (but this is straightforward because they are highly peaked). The method derived in [13] is second order accurate, and the fourth order modified cubic B-spline approximation of Section 5 is a significant improvement. Extension of this approach to modified B-splines with $m > 3$ is work in progress.

REFERENCES

1. A. Bamberger and T.Ha. Duong, *Formulation variationnelle espace–temps pour le calcul par potentiel retardé de la diffraction d'une onde acoustique* (I), Math. Meth. Appl. Sci. **8** (1986), 405–435.

2. L. Banjai, *Multistep and multistage convolution quadrature for the wave equation: algorithms and experiments*, SIAM J. Sci. Comp. **32** (2010), 2964–2994.

3. L. Banjai and Ch. Lubich, *An error analysis of Runge-Kutta convolution quadrature*, BIT **51** (2011), 483–496.

4. L. Banjai, Ch. Lubich and J M Melenk, *Runge-Kutta convolution quadrature for operators arising in wave propagation*, Numer. Math. **119** (2011), 1–20.

5. H. Brunner, *Discretization of Volterra integral equations of the 1st kind* (II), Numer. Math. **30** (1978), 117–136.

6. _____, *Collocation methods for Volterra integral and related functional equations*, Cambridge University Press, Cambridge, 2004.

7. H. Brunner, P.J. Davies and D.B. Duncan, *Discontinuous Galerkin approximations for Volterra integral equations of the first kind*, IMA J. Numer. Anal. **29** (2009), 856–881.

8. _____, *Global convergence and local superconvergence of first-kind Volterra integral equation approximations*, IMA J. Numer. Anal. **32** (2012), 1117–1146.

9. M. Costabel, *Time-dependent problems with the boundary integral equation method*, in *Encyclopedia of computational mechanics*, E. Stein, R. de Borst and T.J.R. Hughes, eds., John Wiley, New York, 2004.

10. P.J. Davies, *Numerical stability and convergence of approximations of retarded potential integral equations*, SIAM J. Numer. Anal. **31** (1994), 856–875.

11. P.J. Davies and D.B. Duncan, *Numerical stability of collocation schemes for time domain boundary integral equations*, in *Computational electromagnetics*, C. Carstensen, S. Funken, W. Hackbusch, R.W. Hoppe and P. Monk, eds., Springer-Verlag, New York, 2003.

12. _____ , *Stability and convergence of collocation schemes for retarded potential integral equations*, SIAM J. Numer. Anal. **42** (2004), 1167–1188.

13. _____ , *Convolution-in-time approximations of time domain boundary integral equations*, SIAM J. Sci. Comp. **35** (2013),B43–B61.

14. C. De Boor, *A practical guide to splines*, Springer-Verlag, New York, 1978.

15. G. Doetsch, *Guide to the applications of the Laplace and Z-transforms*, Van Nostrand, New York, 1971.

16. V. Domínguez and F.-J. Sayas, *Some properties of layer potentials and boundary integral operators for the wave equation*, J. Integral Equat. Appl. **25** (2013), 253–294.

17. A.A. Ergin, B. Shanker and E. Michielssen, *The plane-wave time-domain algorithm for the fast analysis of transient wave phenomena*, IEEE Ant. Prop. Magazine **41** (1999), 39–52.

18. _____ , *Fast analysis of transient acoustic wave scattering from rigid bodies using the multilevel plane wave time domain algorithm*, J. Acoust. Soc. Amer. **107** (2000), 1168–1178.

19. M. Gläfke, *Adaptive methods for time domain boundary integral equations for acoustic scattering*, Ph.D. thesis, Brunel University, UK, 2013.

20. I.S. Gradshteyn and I.M. Ryzhik, *Table of integrals, series, and products*, 5th ed., Academic Press, Boston, 1994.

21. T. Ha-Duong, *On the transient acoustic scattering by a flat object*, Japan J. Appl. Math. **7** (1990), 489–513.

22. _____ , *On retarded potential boundary integral equations and their discretisation*, in *Topics in computational wave propagation*: *Direct and inverse problems*, M. Ainsworth, et al., eds., Springer-Verlag, New York, 2003.

23. W. Hackbusch, W. Kress and S.A. Sauter, *Sparse convolution quadrature for time domain boundary integral formulations of the wave equation*, IMA J. Numer. Anal. **29** (2009), 158–179.

24. E. Hairer, Ch. Lubich and M. Schlichte, *Fast numerical solution of nonlinear Volterra convolution equations*, SIAM J. Sci. Stat. Comp. **6** (1985), 532–541.

25. H. Holm, M. Maischak and E.P. Stephan, *The hp-version of the boundary element method for Helmholtz screen problems*, Computing **57** (1996), 105–134.

26. W. Kress and S.A. Sauter. *Numerical treatment of retarded boundary integral equations by sparse panel clustering*, IMA J. Numer. Anal. **28** (2008), 162–185.

27. M. López-Fernández and S. Sauter, *A generalized convolution quadrature with variable time stepping*, Inst. Mathematik, University of Zurich, Preprint 17-2011, 2011.

28. _____ , *Generalized convolution quadrature with variable time stepping, Part* II: *Algorithm and numerical results*, Inst. Mathematik, University of Zurich, Preprint 09-2012, 2012.

29. M. Lu, J. Wang, A.A. Ergin and E. Michielssen, *Fast evaluation of two-dimensional transient wave fields*, J. Comp. Phys. **158** (2000), 161–185.

30. Ch. Lubich, *Convolution quadrature and discretized operational calculus*, I Numer. Math. **52** (1988), 129–145.

31. _____ , *On the multistep time discretization of linear initial-boundary value problems and their boundary integral equations*, Numer. Math. **67** (1994), 365–389.

32. G. Monegato, L. Scuderi and M.P. Stanic, *Lubich convolution quadratures and their application to problems described by space-time* BIEs, Numer. Alg. **56** (2011), 405–436.

33. F.W.J. Olver, D.W. Lozier, R.E. Boisvert and C.W. Clark, *NIST handbook of mathematical functions*, Cambridge University Press, Cambridge, 2010.

34. J.M. Ortega, *Numerical analysis*: *A second course*, SIAM, Philadelphia, 1990.

35. John G. Proakis and Dimitris G. Manolakis, *Digital signal processing*: *Principles, algorithms, and applications*, Prentice Hall, Upper Saddle River, NJ, 2007.

36. S. Sauter and A. Veit, *Adaptive time discretization for retarded potentials*, Inst. Mathematik, University of Zurich, Preprint 04-2011, 2011.

37. _____ , *A Galerkin method for retarded boundary integral equations with smooth and compactly supported temporal basis functions, Part* II: *Implementation and reference solutions*, Inst. Mathematik, University of Zurich, Preprint 03-2011, 2011.

38. L.L. Schumaker, *Spline functions*: *Basic theory*, 3rd ed., Cambridge University Press, Cambridge, 2007.

39. I. Terrasse, *Résolution mathématique et numérique des équations de Maxwell instationnaires par une méthode de potentiels retardés*, Ph.D. Thesis, l'École Polytechnique, Palaiseau, 1993.

40. Zongmin Wu and R. Schaback, *Shape preserving properties and convergence of univariate multiquadric quasi-interpolation*, Acta Math. Appl. Sinica **10** (1994), 441–446.

DEPARTMENT OF MATHEMATICS AND STATISTICS, UNIVERSITY OF STRATHCLYDE, 26 RICHMOND ST, GLASGOW, G1 1XH, UK
Email address: **penny.davies@strath.ac.uk**

MAXWELL INSTITUTE FOR MATHEMATICAL SCIENCES, DEPARTMENT OF MATHEMATICS, HERIOT–WATT UNIVERSITY, EDINBURGH, EH14 4AS, UK
Email address: **D.B.Duncan@hw.ac.uk**